

*A major project report*  
On  
**Technical Development and Characterization of Graphene Based  
Impedimetric Biosensor**

*Submitted in the partial fulfillment of the requirements for the award of the  
degree of*

**MASTER OF TECHNOLOGY**

**In**

**NUCLEAR SCIENCE & ENGINEERING**

*Submitted by*

**Prashant Ranjan**

**2k14/NSE/21**

*Under the Guidance of*

**Dr. Nitin Kumar Puri**

Assistant Professor

Delhi Technological University

New Delhi

**Dr. Rajesh**

Principal Scientist

National Physical Laboratory

Delhi



**Department of Applied Physics,  
Delhi Technological University**

*(Formerly Delhi college of Engineering, DCE)*

**Govt. of NCT of Delhi**

Main Bawana Road, Delhi-110042



**CSIR-NATIONAL PHYSICAL LABORATORY**  
(Council of Scientific & Industrial Research)  
Dr. K.S. Krishnan Road, New Delhi-110012 (INDIA)



## CERTIFICATE

This is to certify that the project entitled *“Technical Development and Characterization of Graphene Based Impedimetric Biosensor”* Completed by Mr. Prashant Ranjan, Student of M.Tech, Nuclear Science and Engineering in Applied Physics Department at Delhi Technological University, New Delhi embodies the original work carried out by him under my supervision and guidance. His Work has been found very well for the partial fulfillment of the requirement of the degree of M.Tech.

It is further certified that, the student has developed the project during the period starting from 11<sup>th</sup> January, 2016 to 30<sup>th</sup> June, 2016.

This report has not been submitted in part or full in any other University for award of any other degree or diploma.

**Mr. Prashant Ranjan** is student of good moral character. We wish him success in future.

**(Dr. Rajesh)**

Principal Scientist  
Polymers & Soft materials Section  
Materials Physics & Engineering Division

**Head,**  
HRD Group



Department of Applied Physics  
Delhi Technological University (DTU)

(Formerly Delhi College of Engineering, DCE )

Govt. of NCT of Delhi

Bawana Road, Delhi-110042

**CERTIFICATE**

*This is to certify that the Major Project (AP-811) report entitled “Technical Development and Characterization of Graphene Based Impedimetric Biosensor” is a bonafide work done by Prashant Ranjan bearing Roll No. 2k14/NSE/21, a student of Delhi Technological University, in partial fulfilment of the requirements for the award of Degree in Master of Technology in “Nuclear Science & Engineering”. As per declaration of the student this report has not been submitted in part or full in any other University for award of any other degree or diploma.*

(Prof. S. C. SHARMA)

Head of the department

Deptt. Of Applied Physics,

Delhi Technological University

Delhi-110042

(Dr. NITIN KUMAR PURI)

Assistant Professor,

Co-ordinator, M.Tech (NSE)

Delhi Technological University

Delhi-110042

## **Candidate Declaration**

I hereby declare that the work which is being presented in this thesis entitled **“Technical Development and Characterization of Graphene Based Impedimetric Biosensor”** my own work carried out under the guidance of Dr. Nitin K Puri, Assistant Professor, Applied Physics Department, Delhi Technological University, Delhi And Dr. Rajesh, Principal Scientist National Physical Laboratory, New Delhi.

I further declare that the matter embodied in this thesis has not been submitted for the award of any other degree or diploma.

Date:

Prashant Ranjan

Place: New Delhi

2k14/NSE/21

*Dedicated to*  
*My Parents*

## ACKNOWLEDGEMENT

---

I sincerely thank my guide Dr. Rajesh, Principal Scientist, Liquid Crystal and SAM Section, National Physical Laboratory, New Delhi for his guidance, constant support and encouragement throughout my project.

It is my great respect and profound gratefulness that I record my indebt and deep felt devotion to my supervisors. Dr. Rajesh, Principal scientist, Crystal and SAM section, National Physical Laboratory, New Delhi and Dr. Nitin K. Puri, Assistant Professor , Department of Physics, DTU for their precious and encouraging supervision, valuable discussions and inspiring guidance throughout the work. Despite having a busy work schedule, they helped me a lot throughout this project with great interest. Things that I have learnt from them will continue to guide me further in my academic career.

I would like to extend my thanks to Prof. S. C. SHARMA, Head, Department of Physics, DTU for his kind guidance and support during the course for allowing me to carry out my project work in this esteemed research laboratory, NPL, New Delhi.

I would like to thank to Dr.R.K.Kotnala, Chief Scientist, for his constructive suggestions, constant inspiration and timely help. Also I would like to thank to Mr. Vikash sharma, Mr. V.K. Tanwar, Mr. Mangeram for their guidance and help at each and every step of my project. Besides my advisor, I would like to thank the rest of my thesis committee: Shobhita Singal, Who rescued me from various red tape crises and reviewed my work on a very short notice and Jitender Kumar for assistance and encouragement. I am grateful for the whole Liquid Crystal and SAM section for providing me all the facilities to complete my work.

I am extremely thankful to Dr. D.K.Aswal, Director, National Physical Laboratory, New Delhi, For his Kind Permission to carry out the project work at NPL. I express my sincere thanks to Dr. Rajeev Chopra, HRD group NPL, for allowing me to do my M.Tech research Project at NPL.

I heartedly thank to my classmates for their support during my studies.

With deep sense of gratitude, I recorded here my happiness in thanking to my parents with continuous presence and inspirations which guided me all along in developing this project work.

Prashant Ranjan  
2k14/NSE/21

# Table of Contents

Title	Page No
List of Figure and Tables	
Abstract	
CHAPTER-1 .....	1
INTRODUCTION .....	1
1.1 Biosensor.....	2
1.2 Generation of Biosensor .....	4
1.3 Bioreceptors .....	7
1.3.1 Antibody/Antigen Interaction.....	8
1.3.2 Nucleic Acid Interaction.....	11
1.3.3 Enzyme Interaction.....	11
1.3.4 Cellular Interaction .....	13
1.3.5 Interactions using Biometric Materials.....	14
1.4 Transducers .....	15
1.4.1 Optical Techniques .....	15
1.4.2 Electrochemical detection methods .....	16
1.4.3 Mass detection methods.....	17
1.5 Types of Biosensors .....	17
1.5.1 Resonant Biosensors.....	17
1.5.2 Optical-detection Biosensors .....	17
1.5.3 Thermal-detection Biosensors .....	18
1.5.4 Ion-Sensitive Biosensors .....	18
1.5.5 Electrochemical Biosensors.....	18
1.5.5.1 Conductimetric.....	19
1.5.5.2 Amperometric .....	19
1.5.5.3 Potentiometric .....	19
1.5.6 Glucose Biosensors.....	19
1.6 Immobilization of Biological Recognition Element.....	21
1.6.1 Adsorption.....	21

1.6.2	Entrapment.....	21
1.6.3	Microencapsulation .....	22
1.6.4	Crossing-Linking.....	22
1.6.5	Covalent Binding .....	22
1.7	Immunosensors.....	22
1.8	Linear Sweep and Cyclic Voltammetry .....	23
1.9	Electrochemical Impedance Spectroscopy(EIS) .....	25
1.10	Nyquist Plot .....	25
1.11	Bode Plot .....	27
1.12	Warburg Impedance.....	28
CHAPTER-2.....		30
Materials and Methods.....		30
2.1	Apparatus .....	31
2.2	Cleaning Of GCE .....	31
2.3	Graphene Formation.....	31
2.4	Preparation of FeCl <sub>3</sub> .....	31
2.5	Etching .....	31
2.6	Synthesis of PBS Buffer Solution .....	32
2.7	Preparation of Redox.....	32
2.8	Fabrication of Ab-CRP-DEN/PMA/AT/G/GCE.....	32
2.9	CRP .....	33
2.10	Instrumentation.....	34
CHAPTER-3.....		36
RESULT AND DISCUSSION .....		36
3.1	Electrochemical Characterization of the Bioelectrode.....	37
3.2	EIS of the matrix Ab-CRP/DEN-PMA/ AT/G/GCE .....	38
3.3	Electrochemical Impedance Response to Ag-CRP .....	42
CHAPTER-4.....		46
CONCLUSION.....		46
REFERENCES .....		48



## List of Figures

---

<b>Figure Name</b>	<b>Page No</b>
<b>Figure 1: General concept of a Biosensor</b>	<b>2</b>
<b>Figure 2: 1<sup>st</sup> Generation Biosensors</b>	<b>4</b>
<b>Figure 3: 2<sup>nd</sup> Generation Biosensors</b>	<b>5</b>
<b>Figure 4: 3<sup>rd</sup> Generation Biosensors</b>	<b>5</b>
<b>Figure 5: Different Categories of Biosensors</b>	<b>7</b>
<b>Figure 6: Antigen/Antibody Interactions</b>	<b>8</b>
<b>Figure 7: Classes of Antibodies</b>	<b>9</b>
<b>Figure 8: Structure of Antibody</b>	<b>10</b>
<b>Figure 9: Catalyzed reaction by glucose oxidase</b>	<b>20</b>
<b>Figure 10: Excitation function for a LSV experiment</b>	<b>23</b>
<b>Figure 11: Excitation function for a CV experiment</b>	<b>24</b>
<b>Figure 12: Cyclic voltammetry</b>	<b>24</b>
<b>Figure 13: Nyquist Plot</b>	<b>26</b>
<b>Figure 14: Bode Plot</b>	<b>28</b>
<b>Figure 15: Photograph of autolab instrument model no. PGSTST302N</b>	<b>34</b>
<b>Figure 16: Cyclic voltammetry of the matrix</b>	<b>38</b>
<b>Figure 17: Nyquist Plot of the matrix of electrode GCE</b>	<b>41</b>
<b>Figure 18: Bode Plot (Phase analysis) of the matrix of electrode GCE</b>	<b>41</b>
<b>Figure 19: Bode Plot (impedance analysis) of the matrix of electrode GCE</b>	<b>42</b>
<b>Figure 20: Nyquist Plot response to Ag-CRP at different concentration of electrode GCE</b>	<b>43</b>
<b>Figure 21: Bode Plot (impedance analysis) response to Ag-CRP at different concentration of electrode GCE</b>	<b>45</b>
<b>Figure 22: Bode Plot (Phase analysis) response to Ag-CRP at different concentration of electrode GCE</b>	<b>45</b>
<b>Figure 23: Concentration-dependent Calibration curve for Ab-CRP (BSA)-DEN-PMA/AT/G/GCE</b>	<b>47</b>

---

# List of Table

---

<b>Table 1 EIS characteristics parameter at various stages of surface modification of the electrode of GCE</b>	<b>40</b>
<b>Table 2 EIS characteristics parameters of the bioelectrode on immunoreaction with different concentration of target Ag-CRP GCE</b>	<b>44</b>

## Abstract

---

We report a DEN/PMA/AT/G hybrid based impedemetric sensor for a label-free detection of C-reactive protein (CRP) in normal human serum. Dendrimer Solution containing EDC/S-NHS, attached to Graphene through a molecular linker 1-pyrenemethylamine. Which offer free terminal carboxyl group for the site specific covalent biomolecular immobilization of protein antibody, CRP, through carbodiimide coupling reaction to form a impedemetric biosensor. The impedemetric biosensor was characterized by frequency response analysis, and current-voltage (I-V) characteristic studies. The bioelectrode exhibited a linear response of CRP detection in the range of  $0.01 \mu\text{g mL}^{-1}$  to  $10 \mu\text{g mL}^{-1}$  with a sensitivity of  $21.2 \Omega \text{ cm}^2$  per decade change in normal human serum.



**CHAPTER-1**  
**INTRODUCTION**

## 1.1 Biosensor

Sensors are the devices, with a signal transducer and composed of active sensing material. The part of these two imperative segments in sensors is to transmit the signal with no amplification from a specific compound or from a change in a reaction. Signal produced by the device in the form of electrical, thermal or optical output signals could be converted into digital signals for further processing. One of the methods of classifying sensors is based on these output signals. In electrochemical Sensors electrodes can sense the materials which are present within the host without doing any damage to the host system thus have more advantage over other. On the other hand, Sensors can be extensively arranged into two categories as Chemical Sensors and Biosensors.

An advantage of Biosensor includes high specificity, quick estimation, simplicity, reagent usage is very low and the biological element can be reused. Parts of Biosensors are recognition element, physical transducer and signal processing device. A Recognition Element is the fundamental component of any sensor. It is due to recognition element that a sensor can specifically respond to one or several analytes among a large number of other substances. The association of the analytes with the bioreceptor is designed to produce an effect measured by the transducer, which convert the information into a measurable effect such as an electrical signal. Hence, Biosensors can be classified either by their bioreceptor or their transducer type.

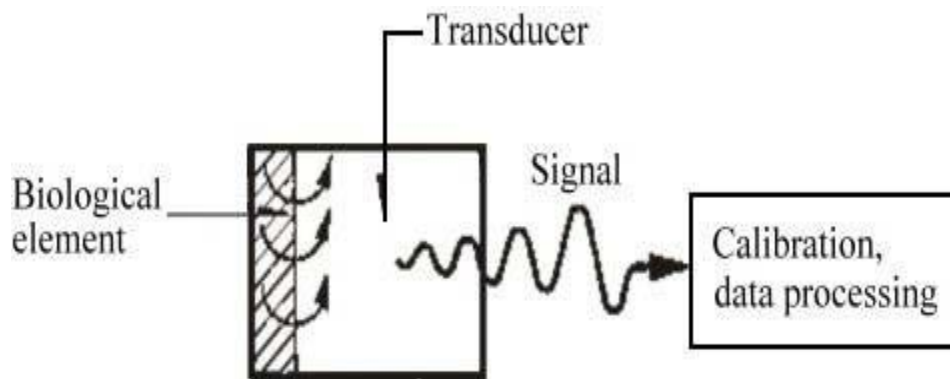


**Figure 1: General concept of a Biosensor**

An effective biosensor must have at least some of the following valuable features:

1. The biocatalyst must be very particular for the analyses, be stable under ordinary storage conditions and, except in the case of colorimetric enzyme strips and dipsticks, indicate good stability over a large number of assays (i.e. much prominent than 100).
2. The response ought to be as independent of such physical parameters as stirring, pH and temperature as is manageable. This would permit the analysis of samples with insignificant pre-treatment. If the reaction involves cofactors or coenzymes these should, ideally, also be co-immobilized with the enzyme.
3. The response should be exact, precise, reproducible and straight over the useful analytical range, without dilution and response must be free from electrical noise.
4. If the biosensor is to be used for invasive monitoring in clinical circumstances, the test must be small and biocompatible, having no toxic or antigenic effects
5. The complete biosensor ought to be cheap, small, portable and capable of being used by semi-skilled operators.

The key part of a biosensor is the transducer which rolls out utilization of a physical change accompanying the response. This might be [1]:-

1. The heat yield (or absorbed) by the reaction (calorimetric biosensors),
2. Changes in the distribution of charges bringing on an electrical potential to be delivered (potentiometric biosensors),
3. Movement of electrons delivered in a oxidation-reduction reaction (amperometric biosensors),
4. light yield during the reaction or a light absorbance distinction between the reactants and products (optical biosensors), or
5. Effects because of to the mass of the reactants or products (piezo-electric biosensors).

## 1.2 Generation of Biosensor

There is three generation of biosensor:

1. First generation, biosensor where the normal product of the reaction diffuses to the transducer and causes the electrical response.

1<sup>st</sup> generation

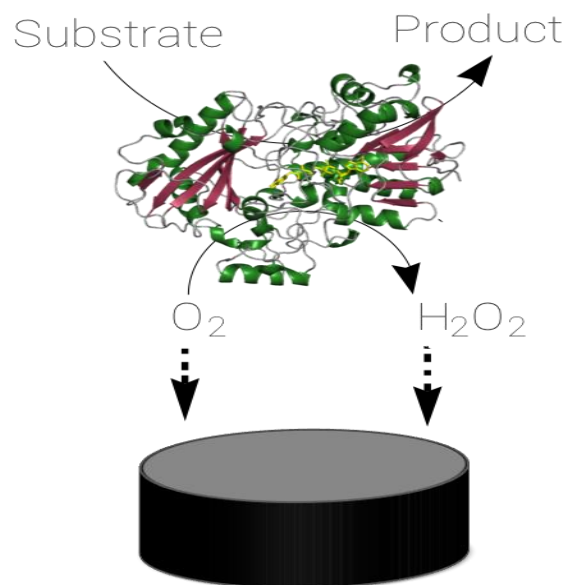


**Figure 2: 1<sup>st</sup> Generation Biosensors**

2. Second generation, biosensors which involve specific “mediators” between the reaction and the transducer in order to generate improved response.



## 2<sup>nd</sup> generation

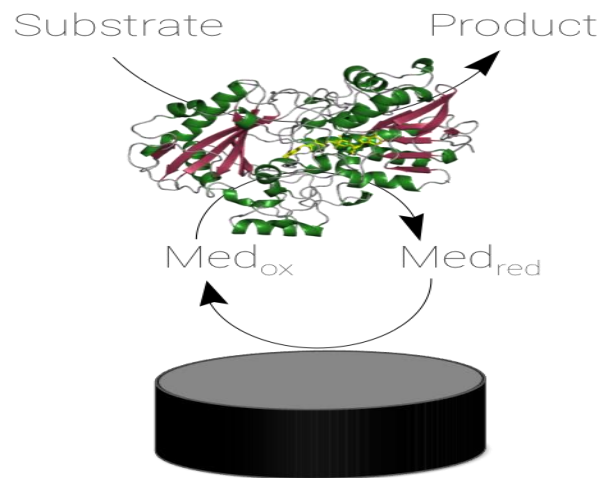


**Figure 3: 2<sup>nd</sup> Generation Biosensors**

3. Third generation, biosensors where the reaction itself causes the response and no product or mediator diffusion is directly involved.

## 3<sup>rd</sup> generation

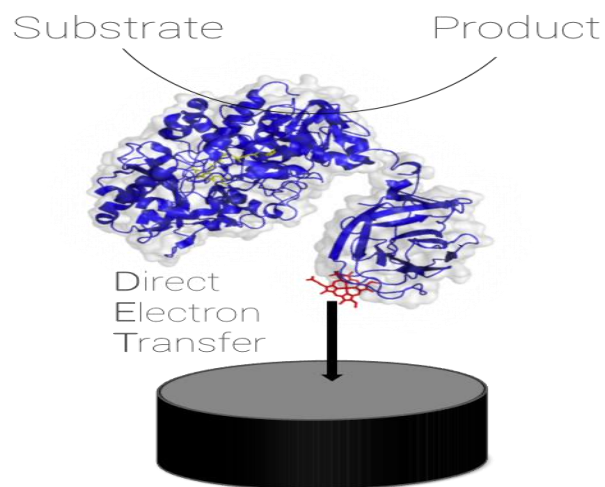


**Figure 4: 3<sup>rd</sup> Generation Biosensors**

The father of the biosensor concept Professor Leland C Clark who invented the first biosensors. At a meeting of the American Society for Artificial Organs amid the yearly meetings of the Federated Societies for Experimental Biology, the biosensor invented was named after him as “Clark electrode” on 15 April 1956. Clark published his complete paper on the oxygen electrode in 1956. The concept was outlined by an analysis in which glucose oxidase was captured at a Clark oxygen electrode using dialysis membrane. This biosensor was created utilizing a thin layer of glucose oxidase (GOx) on an oxygen electrode.

The amount of glucose was evaluated by the reduction in the dissolved oxygen concentration. With the blooming re-launch of the Yellow Springs Instrument Company (Ohio) glucose analyzer based on the amperometric detection of hydrogen peroxide Clark’s ideas became commercial reality in 1975. In 1963 Garry A. Rechnitz together with S. Katz presented one of the first papers in the field of biosensors with the direct potentiometric determination of urea after urease hydrolysis. Around then the term “biosensor” had not yet been coined. Thus, these types of devices were called biocatalytic membrane electrodes or enzyme electrodes. Interestingly, in a glucose biofuel cell enzymes were utilized as fuel cell catalysts by Yahiro in 1964. George Guilbault presented the potentiometric urea electrode in 1969.

Ph. Racine and W. Mindt built up a lactate electrode in 1973. Then came the first microbe-based biosensor in 1976 and finally Karl Cammann presented the term “biosensor” in 1977. Lubbers and Opitz authored the term optode in 1975 to portray a fiber-optic sensor with immobilized marker to quantify carbon dioxide or oxygen. They extended the idea to make an optical biosensor for  $C_2H_5OH$  by immobilising  $C_2H_5OH$  oxidase on the end of a fiber-optic oxygen sensor. Building direct immunosensors by settling antibodies to a piezoelectric or potentiometric transducer had been investigated subsequent to the mid 70’s, but it was a paper by Liedberg that was to pave the way for commercial success. They depicted the utilization of surface plasmon resonance to monitor affinity response in real time.

In 1990 the BI Acore launched is based on this innovation. In 1979 spearheading work by J. Kulys utilizing artificial redox mediators and in 1984 Cass presented first ferrocene-mediated amperometric glucose biosensor which was marketed by MediSense Inc. with a pen-sized meter for home blood-glucose monitoring in 1987. IUPAC presented for the first time definition for biosensors in similarity to the definition of chemosensors in 1997. An enzymatic glucose/ $O_2$  fuel

cell which was embedded in a living plant was introduced by Heller and associates in 2003. The first  $H_2/O_2$  biofuel cell based on the oxidation of low levels of  $H_2$  in air was presented by Armstrong and associates (2006). An embedded glucose biosensor (freestyle Navigator framework) worked for five days.[2]

### 1.3 Bioreceptors

The most common forms of bioreceptors used in biosensing are based on:

1. Antibody/Antigen Interaction.
2. Nucleic Acid Interaction.
3. Enzyme Interaction.
4. Cellular Interaction (i.e. Microorganisms Proteins).
5. Interactions using Biometric Materials (i.e. Synthetic bioreceptors).

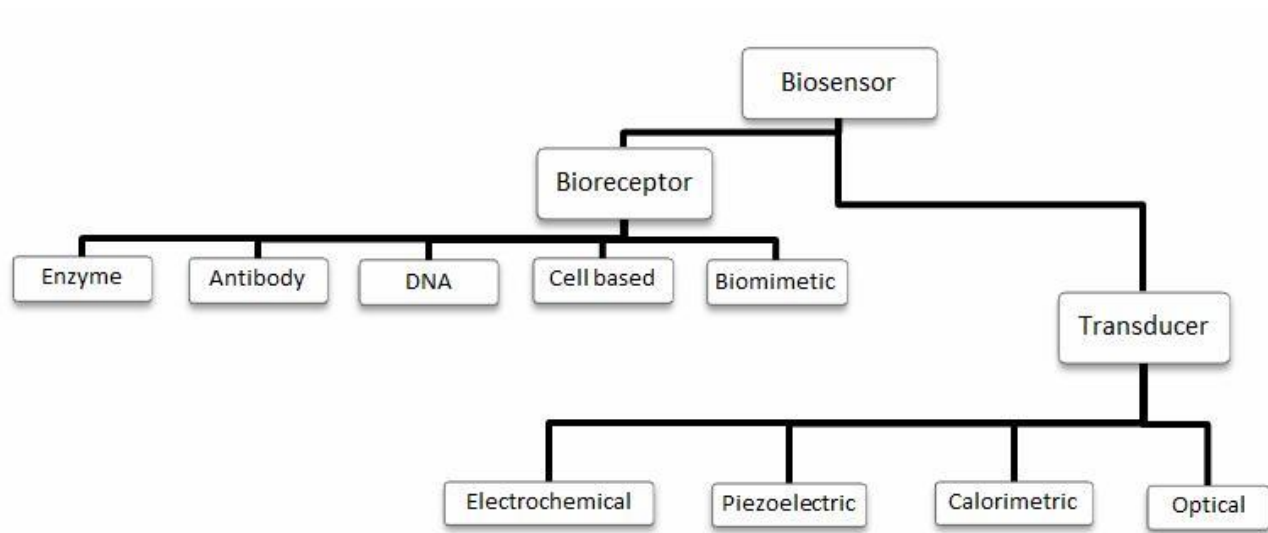


**Figure 5: Different Categories of Biosensors**

### 1.3.1 Antibody/Antigen Interaction

Antibodies, additionally called immunoglobulins, are proteins produced by the body that help fight against foreign substances called antigens. It stimulates the resistant framework to deliver antibodies, when an antigen enters the body. The antibodies join, or tie themselves to the antigen and inactivate it.

Every healthy adult's body has little measures of a large number of various antibodies. Each one is very particular to recognize only one kind of foreign substance. With a binding site on each arm of the Y, antibody molecules are typically Y-shaped,. The binding sites of each antibody, in turn, have a particular shape. Only antigens which match this shape will fit into them. The part of antibodies is to destroy and remove the foreign substances from the body by binding with antigens to inactivate them.

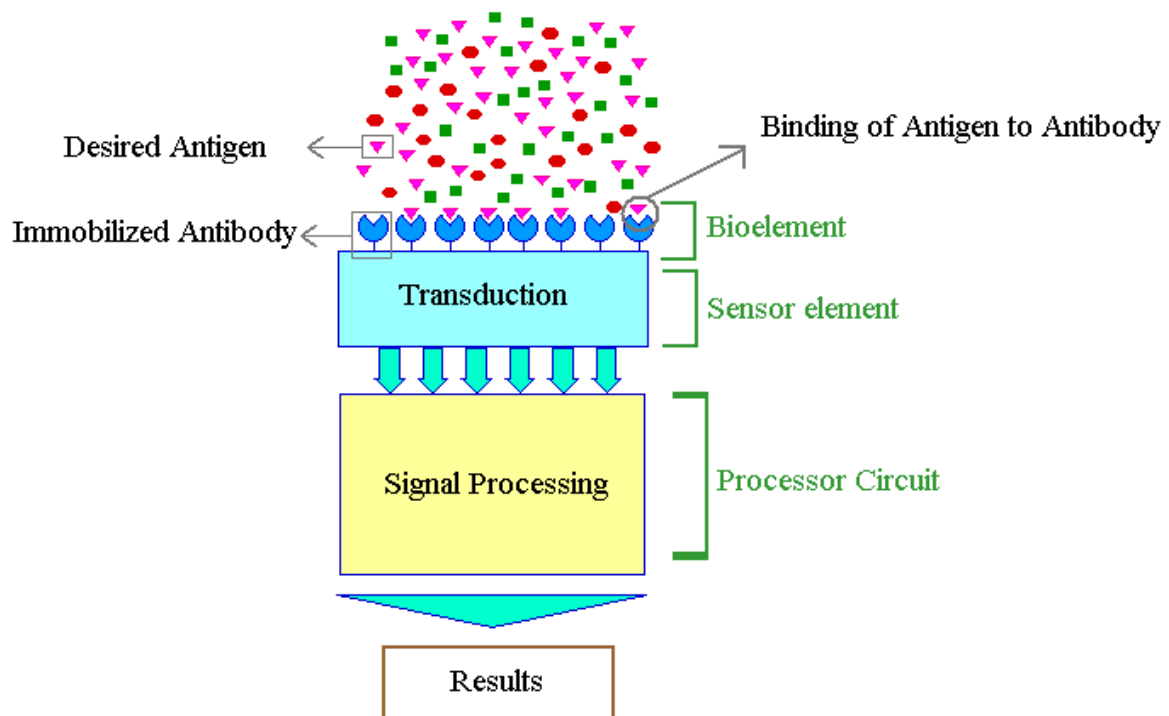


**Figure 6: Antigen/Antibody Interactions**

Antigens are any substance that stimulates the immune system to deliver antibodies. Antigens can be microorganism that causes infection and disease. They can also be substances, called allergens, which bring on an allergic response. It includes dust, pollen, animal dander, bee stings, or certain foods. Blood transfusions containing antigens incongruent with those in the body's own blood will fortify the creation of antibodies, which can cause serious, potentially life-threatening responses.

There are five classes of antibodies, each having a different function. They are IgG, IgA, IgM, IgD, and IgE. Ig is the abbreviation for immunoglobulin, or antibody.

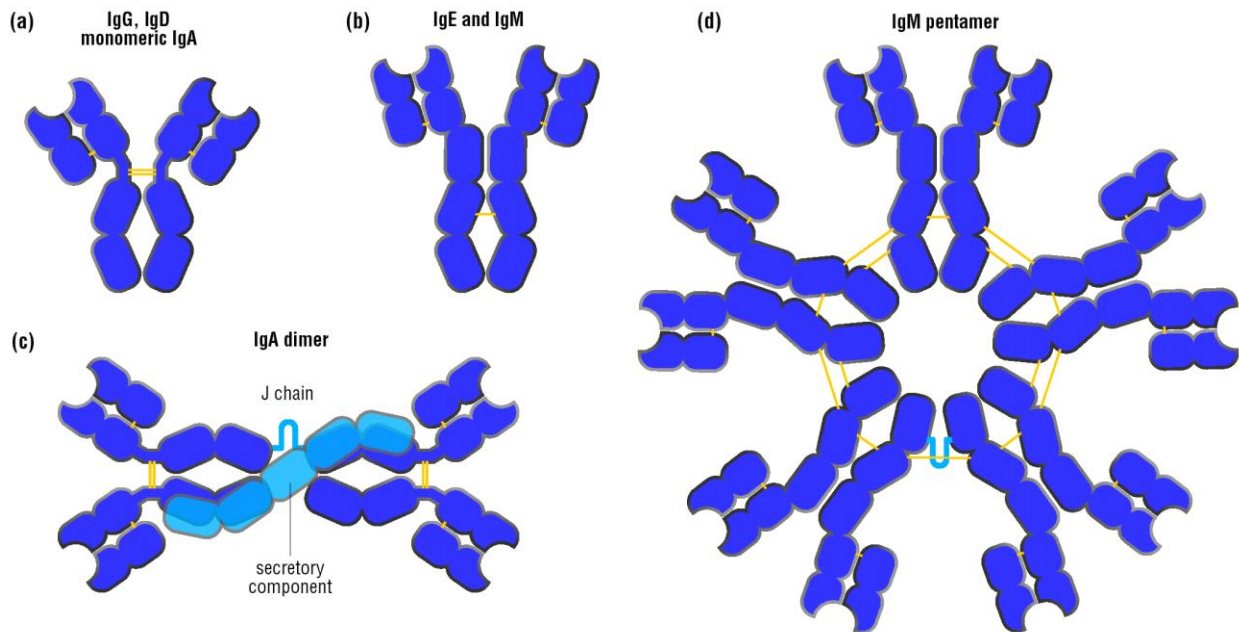


**Figure 7: Classes of Antibodies**

IgG antibodies are the most common and the most important. They circulate in the blood and other body fluids, defending against invading bacteria and viruses. The binding of IgG antibodies with bacterial or viral antigens activates other immune cells that engulf and destroy the antigens. The smallest of the antibodies, IgG moves easily across cell membranes. In humans, this

mobility allows the IgG in a pregnant woman to pass through the placenta to her fetus, providing a temporary defense to her unborn child.

IgA antibodies are present in tears, saliva, and mucus, as well as in secretions of the respiratory, reproductive, digestive, and urinary tracts. IgA functions to neutralize bacteria and viruses and prevent them from entering the body or reaching the internal organs.

IgM is present in the blood and is the largest of the antibodies, combining five Y-shaped units. It functions similarly to IgG in defending against antigens but cannot cross membranes because of its size. IgM is the main antibody produced in an initial attack by a specific bacterial or viral antigen, while IgG is usually produced in later infections caused by the same agent.

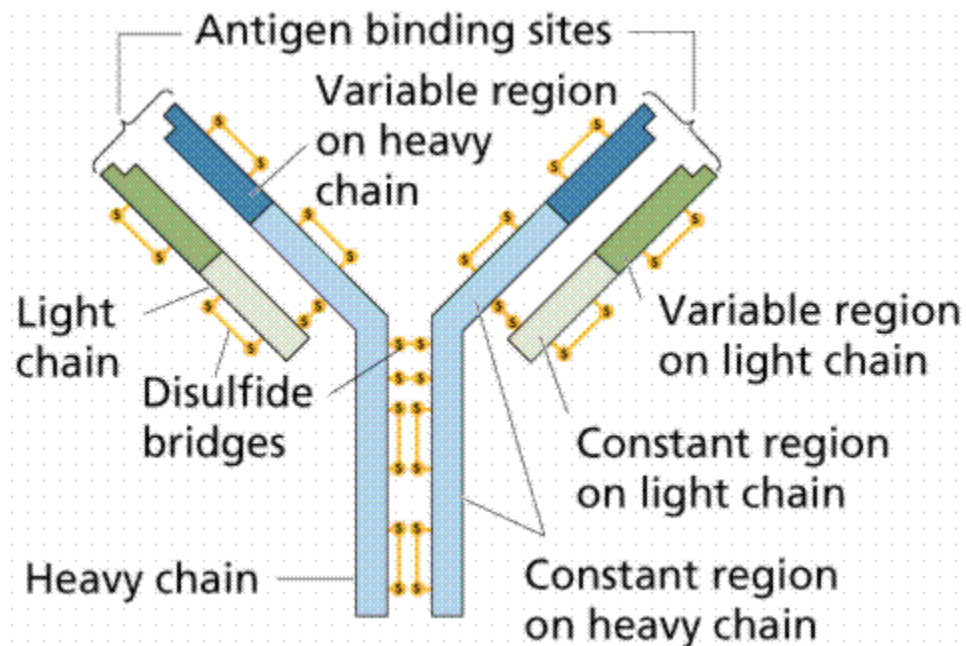


**Figure 8: Structure of Antibody**

### **1.3.2 Nucleic Acid Interaction**

Another biorecognition mechanism includes hybridization of DNA or RNA. In the most recent decade, interest in nucleic acids as bioreceptors for biosensor and biochip advancement has expanded.

The basis for the specificity of biorecognition in DNA biosensors, often referred to as genosensors is formed by the complementarity of the pairing of the nucleotides adenine:thymine and cytosine:guanine in a DNA ladder. The complementary sequence, often called a probe, can be synthesized and labeled with an optically detectable compound if the sequence of bases composing a certain part of the DNA molecule is known. By unwinding the two folded-stranded DNA into single strands, including the probe, and then annealing the strands, the labeled probe can be made to hybridize to its complementary arrangement on the target molecule. The use of DNA biosensors for monitoring DNA–ligand interactions have been reported by Grabley and associate. For monitor real-time binding of low atomic-weight ligands to DNA fragments that were irreversibly bound to the sensor surface via Coulombic interactions surface plasmon resonance technique was used and capable of detecting binding effects between 10 and 400pg/mm<sup>2</sup>.By changing the ligand concentration affinity constants, association rates, dissociation rates, binding rates and equilibrium coverages were calculated for various ligands.

Sandwich-type biosensors based on liquid-crystalline dispersions formed from DNA-polycation complexes have been described by Yevdokimov and co-workers. These sandwich biosensors have been shown to be useful for detection of compounds and physical factors that affect the ability of specific DNA cross linkers polycationic molecules to bind between adjacent DNA molecules.

### **1.3.3 Enzyme Interaction**

Enzymes are frequently utilized as bioreceptors because as a result of their particular binding capabilities and their catalytic activity. In biocatalytic recognition system, the detection is intensified by a catalytic response. This is the premise for the now typical enzyme-linked immunosorbent assay (ELISA) technique.

Except for a small group of catalytic ribonucleic acid particles, all enzymes are proteins. A few enzymes require no chemical groups other than their amino acid residues for activity. Others require an extra segment called a cofactor, which might be it is possible that one or more

inorganic ions, for example  $\text{Fe}^{2+}$ ,  $\text{Mg}^{2+}$ ,  $\text{Mn}^{2+}$ ,  $\text{Zn}^{2+}$ , or a more complex organic or organometallic molecule called a coenzyme. The catalytic activity given by enzymes permits to much lower breaking point of recognition than would be acquired with common binding system. Obviously, the catalytic activity of enzymes relies on the integrity of their native protein conformation. If an enzyme is denatured, separated into its subunits, or into its segment amino acids, its catalytic activity is destroyed. Enzyme-coupled receptors can likewise be utilized to change the recognition mechanisms. For example, the activity of an enzyme can be adjusted when a ligand binds at the receptor. This enzymatic activity is often incredibly improved by an enzyme cascade, which prompts complex responses in the cell.

Gauglitz and associates have immobilized enzymes onto a variety of optical fibers for use in the synchronous recognition of penicillin and ampicillin. These biosensors give an interferometric strategy for measuring penicillin and ampicillin based on pH changes amid their hydrolysis by penicillinase. Immobilized onto the fibers with the penicillinase is a pH marker, phenol red. Shifts in the reflectance range of the pH marker are measured, as the enzyme hydrolyzes the two substrates. Different sorts of data analysis of the spectral information were assessed utilizing a multivariate calibration technique for the sensor array, which comprised of various biosensors. Rosenzweig and Kopelman described the improvement and utilization for the detection of glucose by a micrometer-sized fiber-optic biosensor. These biosensors are 100 times smaller than existing glucose optodes and represent the start of another trend in nanosensor innovation. The oxidation of glucose and oxygen into gluconic acid and hydrogen peroxide was catalyzed by the enzymatic response of glucose oxidase. To monitor the response, an oxygen marker, tris(1,10-phenanthroline)ruthenium chloride, is immobilized into an acrylamide polymer with the glucose oxidase, and this polymer is appended to the optical fiber by means of photopolymerization. A comparison of the reaction of glucose sensors created on various sizes of fibers found that the micrometer-size sensors have response times at least 25 times faster than the larger fibers. In addition, these sensors are accounted for to have absolute detection limits of approximately 10 to 15 mol and an absolute sensitivity five to six orders of magnitude greater than current glucose optodes.

A fiber-optic transitory wave immunosensor for the recognition of lactate dehydrogenase has been developed. Two distinctive measure techniques, a one-stage and a two-stage process, utilizing the sensor based on polyclonal antibody response acknowledgement were depicted. The



reaction of this fleeting wave immunosensor was then compared with an economically available SPR-based biosensor for lactate dehydrogenase detection using similar procedure, and comparative results were obtained. It was also demonstrated that, in spite of the fact the same polyclonal antibody can be utilized for the one- and the two stage process, the two-step technique is significantly better when the antigen is large.[4]

#### **1.3.4 Cellular Interaction**

Microorganisms provide a layout of bioreceptor that generally allows a complete class of compounds to be monitored. Usually these microorganism biosensors depend on the uptake of some chemicals into the microorganism which are used for digestion. Generally, a category of chemicals is ingested by a microorganism which results in allowing a class-specific biosensor to be created. Microorganisms, for example bacteria and fungi have been utilized as indicators of toxicity or for the measurement of specific substances. For example, to evaluate the effects of toxic heavy metals, cell metabolism, cell respiration, and bacterial bioluminescence have been utilized. Many cell organelles can be separated and used as bioreceptors. Cell organelles are mainly closed systems, so they can be used over long periods of time. In bioreceptors, complete mammalian tissue slices cultured mammalian cells have been used as biosensing elements. Plant tissues are also utilized in plant-based biosensors and are mainly catalysts because of the enzymatic pathways they include.

Bilitewski and associates have created a microbial biosensor for monitoring short-chain fatty acids in milk. In a calcium-alginate gel on an electrode surface, *Arthrobacter nicotianae* microorganisms were immobilized. To this gel, 0.5 mM CaCl<sub>2</sub> was included to help in stabilizing it. Monitoring the oxygen consumption of the *A. nicotianae* electrochemically allowed its respiratory activity to be monitored, which provides an indirect means of monitoring fatty acid consumption. Confirmation of short-chain fatty acids in milk which ranges from 4 to 12 carbons in total, was accompanied with butyric acid as the main substrate. A linear dynamic range from 9.5 to 165.5 μM was reported with a response time of 3 min.

Many proteins found within cells mainly serve the motive of bioreception for intracellular reactions which will take place later in different part of the cell. These proteins could easily be utilized for transportation of a chemical from one place to another, for example, a carrier protein or channel protein on a cellular surface. In any case, this protein gives a means of molecular

recognition through one or another type of process (i.e., active site or potential sensitive site). By adding these proteins to different types of transducers, many researchers have found biosensors which depend upon nonenzymatic protein biorecognition.

Cusanovich and associates have found micro- and nanobiosensors for nitric oxide that are free from many potential interferents in one recent research. These sensors are relying on bioreception of nitric oxide by cytochrome *c'*. Two different methods of immobilization of the cytochrome *c'* to fibers were checked. The cytochrome utilized in this work was named with a fluorescent dye that is excited through an energy transfer from the hemoprotein and the response times of faster than 1 s were stated with a detection limit of 20  $\mu M$ . Cytochrome *c'* samples from three different species of bacteria were calculated. Vogel and co-workers have stated on the use of lipopeptides as bioreceptors for biosensors. A lipopeptide have an antigenic peptide segment of VP1, a capsid protein of the picornavirus that causes foot-and-mouth diseases in cattle, was calculated as a method for monitoring antigen–antibody interactions. The protein was defined via circular dichroism and infrared spectroscopy to check that upon self-assembly onto a solid surface it has the same structure as in its free form. Based on surface plasmon resonance measurements, it was seen that the protein was still completely accessible for antibody binding. This method could give an effective means of developing biomimetic ligands for connecting to cell surfaces [6].

### **1.3.5 Interactions using Biometric Materials**

A receptor fabricated and created to mimic a bioreceptor is generally named as a “biomimetic receptor”. Many different ways have been found over the years for the creation of biomimetic receptors. These ways include genetically engineered molecules, artificial membrane fabrication, and molecular imprinting. The molecular imprinting method comprised of mixing analyte molecules with monomers and a large number of cross linkers and has recently get great interest. After polymerization, the hard polymer is ground into a powder and the analyte molecules are taken with organic solvents to remove them from the polymer network. As a conclusion, the polymer has molecular holes or connecting sites that are complementary to the decided analyte. Recombinant techniques, which allow for the synthesis or modification of a wide variety of binding sites using chemical means, have given powerful tools for designing synthetic bioreceptors with desired characteristics. For monitoring phosphorylcholine, Hellinga and

associates stated the creation of a genetically engineered single-chain antibody fragment. In this project, protein engineering methods are utilized to fuse a peptide order which mimics the connecting properties of biotin to the carboxyterminus of the phosphorylcholine-binding fragment of IgA. After this, genetically engineered molecule can be included to a streptavidin monolayer and total internal reflection fluorescence was utilized to control the connecting of a fluorescently named phosphorylcholine analog.

## **1.4 Transducers**

Biosensors can also be divided into many types depending upon the transduction methods they have. Transduction can be accompanied through great types of techniques. Many types of transduction can be classified in one of three main categories which are as.

- 1) Optical detection methods,
- 2) Electrochemical detection methods and
- 3) Mass detection methods.

Therefore, new methods of transducers are continuously being created for use in biosensors.

Each of these three main categories has many different sub categories which creates approximately infinite number of possible transduction techniques or combination of techniques [3].

### **1.4.1 Optical Techniques**

Optical transduction provides the biggest number of possible subcategories of all three of the transducer categories. This is due to the reason that optical biosensors can be utilized for many types of spectroscopy with changing spectrochemical characteristics received. These characteristics have amplitude, energy, polarization, decay time and phase [4-13]. Amplitude is generally measured parameter for the electromagnetic spectrum as it can be connected with the amount of the analyte of interest. Information about varying in the local environment surrounding the analyte, its intramolecular atomic vibrations or the formation of new energy levels can be taken by the energy of the electromagnetic radiation measured. Calculation of the interaction of a free molecule with a fixed surface can generally be known depending upon polarization calculation. Polarization of emitted light is generally random when taken from a free molecule in solution. Therefore, when a molecule bounds to a fixed surface, the emitted light

generally remains polarized. The decay time of a particular emission signal can also be utilized to receive information about the molecular interactions since these decay times are very rely upon the excited state of the molecules and their local molecular environment. The development of a phase-resolved fiberoptic fluoro immune sensor (PR-FIS) has been stated by Vo-Dinh and associates, which can distinguish the carcinogen benzo [a] pyrene and its metabolite benzopyrene tetrol, rely on the difference of their fluorescence lifetimes. Another characteristic that can be considered is the phase of the emitted radiation. When electromagnetic radiation interacts with a surface, the speed or phase of that radiation is varied, based on the refractive index of the medium which is generally analyte. When the medium is varied through connecting of an analyte, the refractive index may vary resulting in change in the phase of the impinging radiation.[14]

#### **1.4.2 Electrochemical detection methods**

Electrochemical detection is a different way of transduction which has been utilized in biosensors [15-17]. This method is very integral part of optical detection methods which are as fluorescence, which is the main sensitive of the optical methods. Since, different analytes of interest are not fluorescent and naming a molecule with a fluorescent name is generally labor intensive, electrochemical transduction can be very beneficial. By connecting the sensitivity of electrochemical calculations with the selectivity given by bioreception, detection limits comparable to fluorescence biosensors are generally obtainable.

Cammann and associates found electrochemical flow-through enzyme-based biosensors for the detection of glucose and lactate. Glucose oxidase and lactate oxidase were immobilized in conducting polymers obtained from pyrrole, N-methylpyrrole, aniline and o-phenylenediamine. These different sensor matrices were comparably based on amperometric calculations of glucose and lactate. It was seen that the o-phenylenediamine polymer was mainly sensitive. This polymer matrix was also accumulated on a piece of graphite felt and utilized as an enzyme reactor as well as a working electrode in an electrochemical detection system.

### **1.4.3 Mass detection methods**

Another method of transduction which has been utilized for biosensors is the calculation of small varies in mass. This is the latest of the three categories of calculations; therefore, it has already been presented to capable of very sensitive calculations. The main motive means of mass analysis depends upon the use of piezoelectric crystals. These crystals can be obtained to vibrate at a particular frequency with the advantage of an electrical signal of a particular frequency [18,19].

Hence, the frequency of oscillation depends upon the electrical frequency applied to the crystal as well as the crystals mass. Thus, when the mass increases due to connection of chemicals, the oscillation frequency of the crystal varies and the resulting vary can be evaluated electrically and be utilized to calculate the extra mass of the crystal. For the detection of *Listeria monocytogenes*, Guilbault and associates have developed a quartz crystal microbalance biosensor. On the surface, through a gold film many different methods were evaluated for immobilization of *Listeria* onto the quartz crystal. The microbalance was placed in a liquid flow cell after getting bound, where the antibody and antigen were allowed to complex, and calculations were achieved.

## **1.5 Types of Biosensors**

Some common types of biosensors are discussed which are as:

### **1.5.1 Resonant Biosensors**

An acoustic wave transducer is coupled with an antibody in this type of biosensor. When the analyte molecule get connect to the membrane, the mass of the membrane changes. Thus, the resulting change in the mass subsequently varies the resonant frequency of the transducer. This frequency varies is then obtained.

### **1.5.2 Optical-detection Biosensors**

The output transduced signal that is obtained is light for optical detection biosensor. The biosensor can be made relying on optical diffraction. In optical diffraction depending devices, a silicon wafer is coated with a protein through covalent bonds. The silicon coated wafer is then kept to Ultra Violet light through a photo-mask and the antibodies gets passive in the exposed regions. Antigen-antibody bindings are formed in the active regions when the diced wafer chips are incubated in an analyte which creates a diffraction grating. This grating generates a

diffraction signal when lightened with a light source for example laser. The resulting signal can be calculated or can be further amplified before measuring for better sensitivity.[5]

### **1.5.3 Thermal-detection Biosensors**

Thermal Detection Biosensor is exploiting one of the basic characteristics of biological reactions, namely absorption or production of heat, which in result varies the temperature of the medium in which the reaction takes place. With temperature sensors, they are created by adding immobilized enzyme molecules. The heat reaction of the enzyme is measured and is calibrated against the analyte quantity when the analyte gets in contact with the enzyme. The total heat generated or absorbed corresponds to the molar enthalpy and the total number of molecules in the reaction. The calculation of the temperature is typically accompanied through a thermistor and these type of devices are known as enzyme thermistors. Their high sensitivity to thermal variation results in thermistors ideal for such applications. Thermal biosensors do not need regular recalibration and are insensitive to the optical and electrochemical characteristics of the sample unlike other transducers. Common characteristics of this type of biosensor involve the detection of pesticides and pathogenic bacteria.

### **1.5.4 Ion-Sensitive Biosensors**

Ion Sensitive Biosensors are semiconductor FETs having an ion-sensitive surface. The surface electrical potential changes when the ions and the semiconductor interact. This variation in the potential can be correspondingly calculated. The Ion Sensitive Field Effect Transistor (ISFET) can be build by bounding the sensor electrode with a polymer layer. This polymer layer is desirably penetrable to 4 analyte ions. The ions penetrate through the polymer layer and results in varying the FET surface potential. This type of biosensor is also called an Enzyme Field Effect Transistor and is basically utilized for pH detection.

### **1.5.5 Electrochemical Biosensors**

Electrochemical biosensors are primarily utilized for the sensing of hybridized DNA, DNA-binding drugs, glucose concentration, etc. The principle for this category of biosensors is that many chemical reactions generate or consume ions or electrons which in result create some variations in the electrical characteristics of the solution which can be detected out and utilized as measuring parameter. Electrochemical biosensors can be further divided based upon the measuring electrical parameters which are as:

- (1) conductimetric,
- (2) amperometric and
- (3) potentiometric.

#### **1.5.5.1 Conductimetric**

The calculated parameter is the electrical conductance or resistance of the solution. The overall conductivity or resistivity of the solution varies when electrochemical reactions generate ions or electrons. This variation is calculated and adjusted to appropriate scale. Conductance calculations have approximately low sensitivity. The electric field is produced using a sinusoidal voltage which is AC and helps in reducing undesired results which are as Faradaic processes, double layer charging and concentration polarization.

#### **1.5.5.2 Amperometric**

This high sensitivity biosensor can sense electroactive species which lies in biological test samples. Since these samples may not be intrinsically electro-active, enzymes are required to catalyze the generation of radio-active species. In such cases, the calculated parameter is current.

#### **1.5.5.3 Potentiometric**

In this category of sensors, the calculated parameter is oxidation or reduction potential of an electrochemical reaction. The basic working principle depends on the issue that when a ramp voltage is put across an electrode in solution, current flow because of the electrochemical reactions. The voltage at which these reactions take place tells a specific reaction and species.

#### **1.5.6 Glucose Biosensors**

Amperometric glucose biosensors are the major commercially successful biosensors. These biosensors have been developed in the market available in different shapes such as glucose pens, glucose displays etc. The invention of glucose biosensors was done by Leland C. Clark which was considered as the first historic experiment. He utilized platinum electrodes to sense oxygen. The enzyme glucose oxidase was put very near to the surface of platinum by physically trapping it in compete with the electrodes with a piece of dialysis membrane. The enzyme activity varies relying on the surrounding oxygen amount Fig.9 presents the reaction catalyzed by glucose oxidase.[20]

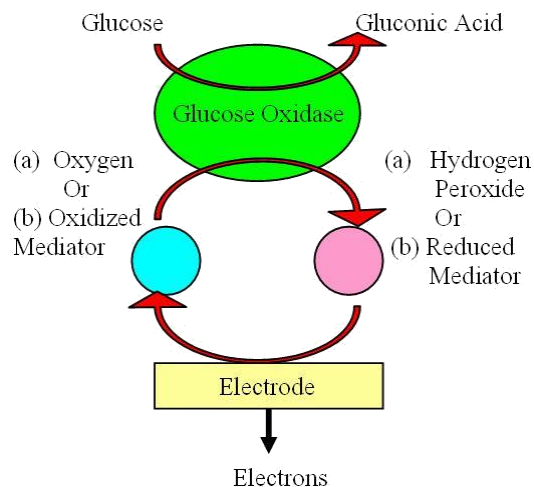


**Figure 9: Catalyzed reaction by glucose oxidase**

Glucose when added with glucose oxidase to produce gluconic acid while generating two electrons and two protons, hence declines glucose oxidase. The declined glucose oxidase covering oxygen, protons and electrons which are produced earlier add to produce hydrogen peroxide and oxidized glucose oxidase in the original form. This glucose oxidase can again add with more glucose quantity. The larger the glucose quantity, higher oxygen is utilized. On another side, smaller glucose quantity results in higher hydrogen peroxide. Therefore, either the utilization of oxygen or the generation of hydrogen peroxide can be sensed by the platinum electrodes and this can be used as a measure for glucose concentration. Disposable amperometric biosensors for the detection of glucose are also available. The difficult structure is a button-shaped biosensor comprised of the given layers which are as metallic substrate, graphite layer, isolating layer, mediator modified membrane, immobilized enzyme membrane i.e. glucose oxidase and a cellulose acetate membrane. This biosensor utilized graphite electrodes not platinum electrodes. The separating layer is put on the graphite electrodes which can filter out some interfering acids such as ascorbic acid, uric acid with allowing the path of hydrogen peroxide and oxygen. The advanced mediator membrane aids in keeping the glucose oxidase membrane to the graphite electrode when the electrochemical reaction takes place at a particular given voltage. A barrier for interfering substances has been provided by the cellulose acetate outer layer placed over the glucose oxidase. The amperometric reading of the biosensor which is current versus glucose quantity figures that the relationship is linear up to a particular glucose quantity. In another words, we can say that current increases linearly with glucose quantity; therefore it can be



utilized for sensing. The current and future applications of glucose biosensors are very wide due to their utilization in diabetic self-monitoring of capillary blood glucose. This type of monitoring devices consists one of the biggest markets for biosensors today and their existence has correspondingly enhanced the quality of life of diabetics.

## **1.6 Immobilization of Biological Recognition Element**

The biological recognition element has to be properly attested to the transduction element in order to create a biosensor. In the creation of immobilizing biological recognition element onto the sensor surface, progress has been made considerably. There are five main techniques which are utilized for immobilization of recognition element and are discussed as follows:

### **1.6.1 Adsorption**

Solid Phase Substrates for example alumina, charcoal, silica gel and glass can be absorbed by some molecules. There is no need for clean-up step with low disruption to the biomolecules. Also, no reagents are required for the same. Adsorption can be categorized further into two methods which are as physical adsorption and chemical adsorption. **Physical adsorption** is generally weak and happens via the production of electrostatic interactions, Van Der Waals bonds, or hydrogen bonds. **Chemical adsorptions** are very stronger and have the production of covalent bonds. To prepare a sensing surface with lesser preparation, adsorption is the easiest technique. Therefore, the absorbed biomolecules are very easily able to vary in pH, ionic strength, temperature and the substrate. Thus, for short-term investigations, this technique is only suitable.

### **1.6.2 Entrapment**

The biomolecules are mixed with monomer solution which is polymerized to a gel in this immobilization scenario. The biomolecules are therefore fixed within the gel matrix. The main polymer which is utilized commonly is polyacrylamide. Some another materials such as starch gels, silastic gels and nylon are also utilized in this technique. Conducting polymers for example polypyrroles are specifically useful for electrode based surface because of their unique electric characteristics. The problems connected with this technique are generally restrictions for the penetration of desired analyte to the receptors and loss of bioactivities of the receptors via the pores in the gel.

### **1.6.3 Microencapsulation**

In early biosensor design this technique was generally utilized. The biomolecules are held set up behind a membrane, giving close contact between the receptors and the transducer. The membrane is stable towards changes in pH, temperature and ionic strength. Cellulose acetate, cellophane, polycarbonate and polyurethane are the main types of membranes.

### **1.6.4 Crossing-Linking**

In this strategy, the biomolecules are chemically bound to solid supports or to another supporting material, for example gel Bi-functional reagents such as glutaraldehyde, hexamethylene, diisocyanate and 1,5-dinitro-difluorobenzene are used.

### **1.6.5 Covalent Binding**

This methodology includes a carefully designed bond between a functional group in the receptor to the support matrix and uses nucleophilic groups for coupling. A decent example of this technique is that a carboxyl group on the support reacts with a carbodiimide, trailed by coupling with an amine group on the receptor to form an amide bond between the solid support and the receptor.

## **1.7 Immunosensors**

An immunosensor is a device involving an antigen or antibody species coupled to a signal transducer, which identifies the binding of the reciprocal species. An indirect immunosensor utilizes a different labeled species that is recognized after binding by, e.g., fluorescence or luminescence. A direct device recognizes the binding by a change in potential difference, current, resistance, mass, heat, or optical properties. Although indirect sensors may experience lesser issues because of nonspecific binding effects while the direct sensors are capable of real-time monitoring of the antigen-antibody reaction. An extensive range of molecules can be recognized with detection limits ranging between  $10^{-9}$  and  $10^{-13}$  mol/L. In any case, there are only a few successful business applications of direct immunosensors, these being of the optical type. This survey portrays the principles underlying the technologies, their merits, limitations, and applications. With either antibody or antigen immobilized at the sensor surface such devices are based on the principles of solid-phase immunoassay. Medical diagnostic markers such as hormones, drugs, and bacteria, and environmental pollutants such as pesticides are an extensive range of analytes which can be detected and measured by immunosensors. The ability to investigate the reaction dynamics of antibody-antigen binding has given these devices the

potential to revolutionize conventional immunoassay techniques is the advantages of an absence of labeling requirements.

### 1.8 Linear Sweep and Cyclic Voltammetry

In linear sweep voltammetry (LSV) a fixed potential range is employed much like potential step measurement.

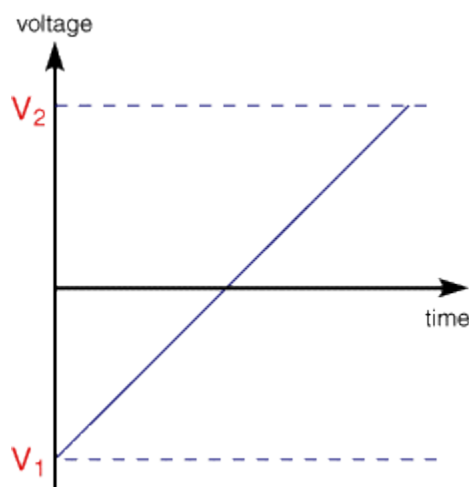


**Figure 10: Excitation function for a LSV experiment**

The characteristics of the linear sweep voltammogram recorded depend on a number of factors including:

1. The rate of the electron transfer reactions.
2. The chemical reactivity of the electro active species.
3. The voltage scan rate.

Cyclic voltammetry (CV) is very similar to LSV. In this case the voltage is swept between two values at a fixed rate.

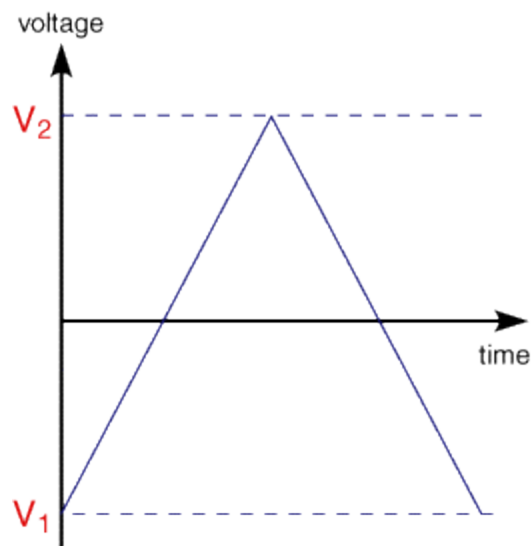


**Figure 11: Excitation function for a CV experiment**

The forward sweep produces an identical response to that seen for the LSV experiment. When scan is reversed we simply move back through the equilibrium positions gradually converting electrolysis product. ( $\text{Fe}^{2+}$  back to reactant  $\text{Fe}^{3+}$ ).

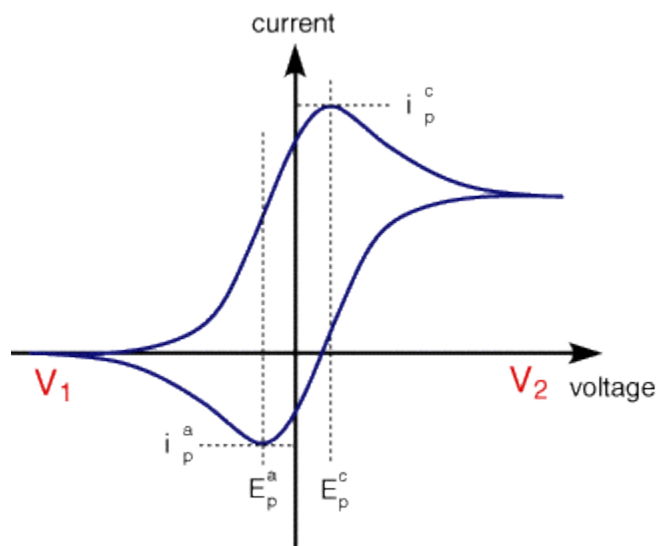


**Figure 12: Cyclic voltammetry**

The current flow is now from the solution species back to the electrode and so occurs in the opposite sense to the forward sweep but otherwise the behavior can be explained in an identical manner.

1. The voltage separation between the current peak

$$\Delta E = E_p^a - E_p^c = \frac{59}{n}mv$$

2. The positions of peak voltage do not alter as a function of voltage scan rate.
3. The ratio of the peak current is equal to one.

$$\left| \frac{I_p^a}{I_p^c} \right| = 1$$

4. The peak currents are proportional to the square root of the scan rate.

$$I_p^a \text{ and } I_p^c \propto \sqrt{v}$$

### **1.9 Electrochemical Impedance Spectroscopy(EIS)**

The EIS type measurement is suitable for real time monitoring since it is able to provide a label free or reagent less detection. In EIS measurement, the sample is placed on the sensing device such as nanogap, and a controlled alternating voltage is applied to the electrode, and the current flows through the sample are monitored. The electrical impedance resulting from the sample is calculated as the ratio of voltage over current. The resulting electrical impedance measurement has both a magnitude and a phase, a complex number. For any time-varying voltage applied, the resulting current can be in phase with the applied voltage (resistive behavior), or out of phase with it (capacitive behavior).

The EIS consists of 3 electrode system, a potentiostats and a frequency response analyzer (FRA). The three electrode which are working electrode that provides the measurement of current, counter electrode that provides current to cell and reference electrode for voltage measurement.

### **1.10 Nyquist Plot**

The Nyquist Plot Figure 8 shows one popular format for evaluating electrochemical impedance data, the Nyquist plot. This format is also known as a Cole-Cole plot or a complex impedance plane plot. In our study, we plotted the imaginary impedance component ( $Z''$ ) against the real impedance component ( $Z'$ ) at each excitation frequency. At high frequencies, the impedance of the Randles cell was almost entirely created by the ohmic resistance,  $R_w$ . The frequency reaches

its high limit at the leftmost end of the semicircle, where the semicircle touches the x axis. At the low frequency limit, the Randies cell also approximates a pure resistance.

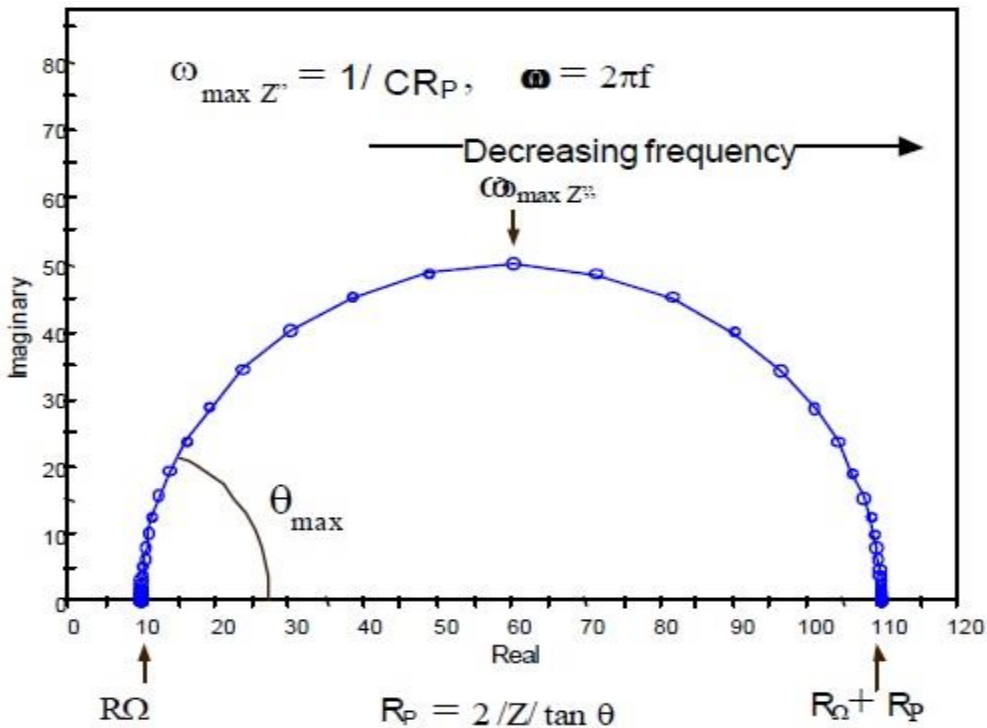


**Figure 13: Nyquist Plot**

The frequency reaches its low limit at the rightmost end of the semicircle. The Nyquist plot has several advantages. The primary one is that the plot format makes it easy to see the effects of the ohmic resistance. If you take data at sufficiently high frequencies, it is easy to extrapolate the semicircle toward the left, down to the x axis to read the ohmic resistance. The shape of the curve (often a semicircle) does not change when the ohmic resistance changes. Consequently, it is possible to compare the results of two separate experiments that differ only in the position of the reference electrode. Another advantage of this plot format is that it emphasizes circuit components that are in series, such as  $R_w$ . The Nyquist plot format also has some disadvantages. For example, frequency does not appear explicitly. Secondly, although the ohmic resistance and polarization resistance can be easily read directly from the Nyquist plot, the electrode capacitance can be calculated only after the frequency information is known. The frequency

corresponding to the top of the semicircle,  $\omega(q = \text{MAX})$ , can be used to calculate the capacitance if  $R_p$  is known. Although the Nyquist format emphasizes series circuit elements, if high and low impedance networks are in series, you will probably not see the low impedance circuit, since the larger impedance controls plot scaling.

### **1.11 Bode Plot**

In impedance spectroscopy, a small sinusoidal voltage is placed on the sample over a wide frequency range, from  $10^5$  to  $10^{-3}$  Hz. It is therefore an alternating current (AC) technique. The controlling computer system measures the magnitude of the current induced by the potential and in addition the phase angle between the potential and current maxima. A modified Ohms law is applied:

For DC conditions:-

$$V = iR$$

For AC conditions:-

$$V = iZ$$

Where  $Z$  is the Impedance of the system

The Bode plot has some distinct advantages over the Nyquist plot. Since frequency appears as one of the axes, it's easy to understand from the plot how the impedance depends on the frequency. The plot uses the logarithm of frequency to allow a very wide frequency range to be plotted on one graph, but with each decade given equal weight. The Bode plot also shows the magnitude ( $|Z|$ ) on a log axis so that you can easily plot wide impedance ranges on the same set of axes. This can be an advantage when the impedance depends strongly on the frequency, as is the case with a capacitor. The Bode plot format also shows the phase angle,  $q$ . At the high and low frequency limits, where the behavior of the Randles cell is resistor-like, the phase angle is nearly zero. At intermediate frequencies,  $q$  increases as the imaginary component of the impedance increases. The  $q$  vs.  $\log \omega$  plot yields a peak at  $\omega (q = \text{MAX})$ , the frequency, in radians, at which the phase shift of the response is maximum.

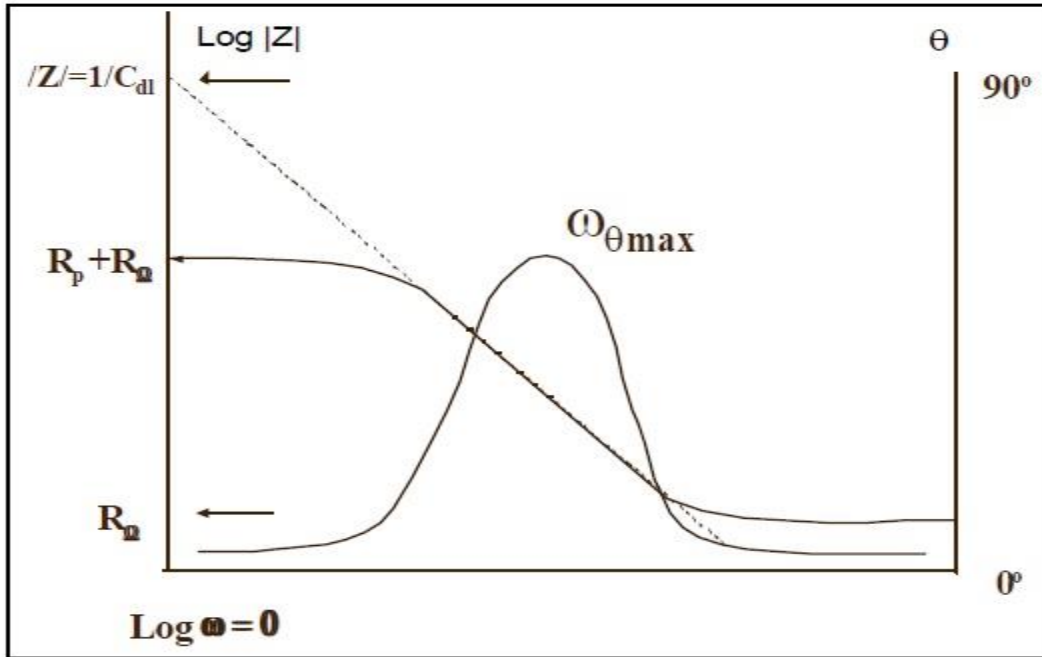
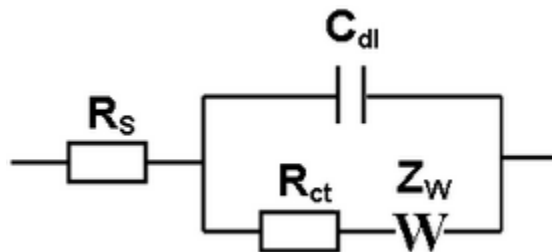


**Figure 14: Bode Plot**

The Bode plot is a useful alternative to the Nyquist plot. It lets you avoid the longer measurement times associated with low frequency. Furthermore, the  $\log |Z|$  vs.  $\log \omega$  plot sometimes allows a more effective extrapolation of data from higher frequencies.

### **1.12 Warburg Impedance**

In electrochemical systems, diffusion of ionic species at the interface is common. The Warburg impedance was developed to model this phenomenon several expressions based on the assumptions are used to describe diffusion impedance. Under the assumption of semi-infinite diffusion layer, the impedance is:





$$Z_w = \frac{1}{Y\sqrt{j\omega}}$$

Where Y is the diffusion admittance.

Warburg impedance is characterized by having identical real and imaginary contributions, resulting in a phase angle of 45°

Based on the nature of the measuring signal, impedance immunosensors can be classified into two main categories.

- a) Capacitive
- b) Faradaic

Warburg impedance describes how the diffusion of the redox probe toward the electrode can influence the current flow and consequently the impedance.

- a) Capacitive:- Electrode surface is completely covered by a dielectric layer and the whole electrode assembly behaves as an insulator. No redox probe is present in the measuring solution and the capacitive current is measured under small amplitude sinusoidal voltage signal, at low excitation frequencies (typically 10-10<sup>3</sup>hz). Ab-Ag interaction are expected to cause a decrease in the measuring capacitance since less polar protein molecule replace water molecules from the electrode surface.
- b) Faradaic:- Where the surface of the electrode, which is partially or fully covered by a non-insulating layer, or partially covered by an insulating layer is able to catalyse a redox probe, which exists in the measuring solution .In the case measuring parameter is the charge transfer resistance and Ab-Ag interactions are expected to cause an increase in its value as the faradaic reaction becomes more hindered.

## **CHAPTER-2**

### **Materials and Methods**

## **2.1 Apparatus**

Cyclic voltammetry (CV) and EIS measurements were done on a PGSTAT302N, AUTOLAB instrument from Eco Chemie, The Netherlands. The EIS parameters were obtained by circuit fitting the EIS experimental data using GPES (General purpose electrochemical system version 4.9, Eco Chemie) software. All electrochemical measurements were carried out in a conventional three-electrode cell configuration consisting of the proposed bioelectrode as working electrode, Ag/AgCl as reference electrode and platinum wire as counter electrode.

## **2.2 Cleaning Of GCE**

Prior to use, the GCE was polished carefully to a mirror like plane with 1, 0.3 and 0.05  $\mu\text{m}$  alumina powder and rinsed with Millipore water, followed by sonication in Millipore water, Ethanol and (1:1) Nitric acid, respectively for 15 min each . Then, the electrode was allowed to dry under  $\text{N}_2$  gas.

## **2.3 Graphene Formation**

Graphene was grown on a Cu foil through CVD method using acetylene as precursor gas. The Cu foil was positioned in the interior of a fused silica tube (5 cm inside diameter by 100 cm long) kept in a heating furnace and the temperature was elevated to  $450^\circ\text{C}$  under, continuous flow of  $\text{Ar}/\text{H}_2$ , 200 sccm (standard cubic centimeter per min)/100sccm, atmosphere, where it was annealed and reduced for 30 minutes in order to recover a pure metal surface. Thereafter, the temperature of the furnace was elevated to  $850^\circ\text{C}$  and a 5 sccm flow of  $\text{C}_2\text{H}_2$  was introduced for 3 minutes, followed by cooling of furnace to room temperature under  $\text{Ar}/\text{H}_2$  atmosphere.

## **2.4 Preparation of $\text{FeCl}_3$**

The solution is prepared using  $\text{FeCl}_3$  as the solute and water as a solvent, for that 16gm of  $\text{FeCl}_3$  is dissolved in 100ml of water. Then centrifuge for 15 at 10,000 RPM then filter.

## **2.5 Etching**

The Cu foil was taken out from the furnace with the graphene grown on one side was protected by Poly (methyl methacrylate) (PMMA), whereas the graphene on the opposite side was burnt off using reactive ion etching (RIE). The above Cu foil was cut into small pieces of desired area ( $3 \times 3 \text{ mm}^2$ ) and was etched in 1M aqueous  $\text{FeCl}_3$  solution to obtain the floating graphene film,

followed by washing repeatedly with distilled water and aqueous 0.1M HCl to remove the metal impurities.

## **2.6 Synthesis of PBS Buffer Solution**

The steps involved for preparation of PBS buffer are:

Prepare 1.0 M buffer solution by making A and B as follows-

A: 0.2 M solution of monobasic potassium phosphate (6.96gm in 200ml water)

B: 0.2 M solution of dibasic potassium dihydrogen phosphate (2.72gm in 100ml water)

19ml of A + 81ml of B +1480 mg of KCL, diluted to a total of 200 ml.

By this we can prepare the stock solution of PBS buffer of PH -7.4.

## **2.7 Preparation of Redox**

Redox probe is prepared in 10ml buffer solution having PH value of 7.4, solute added are  $K_3Fe(CN)_6$  6.5mg and  $K_4Fe(CN)_6$  8.4mg.

## **2.8 Fabrication of Ab-CRP-DEN/PMA/AT/G/GCE**

The graphene film was transferred on GCE surface (3 mm diameter) by careful scooping and rinsed with acetone to remove the PMMA, and dried at 50°C for 1 hr. to obtain the G/GCE. The graphene mounted on GCE was pretreated by anodization at a potential of 1.7 V vs. Ag/AgCl for 500 s in PBS; pH 7.4, followed by cathodization at -0.6 V for 60 s to obtain the porous electroactive graphene (AT/G/GCE). This treatment to graphene introduced defects on the edge planes of graphene with the generation of carbonyl groups during oxidation that were subsequently reduced to C-OH, leading to an enhance electroactive behavior of graphene. The EG was treated with a bilinker, PMA, for the covalent attachment of dendrimer solution (DEN) using carbodiimide coupling reaction. 10  $\mu$ L, 2 mM PMA in DMF, was drop casted on AT/G/GCE and left for 40 minutes at room temperature, followed by washing extensively with DMF and dried under N<sub>2</sub> gas flow to obtain the PMA functionalized EG/GCE through  $\pi$ -  $\pi$  stacking. The carboxyl groups of dendrimer nanoparticles were activated into corresponding ester by using EDC and NHS for carbodiimide coupling reaction partially with active amino group of PMA for effective covalent attachment on EG/GCE and the remaining on the other

hand with active amino group of the CRP molecules for covalent biomolecular immobilization. Aqueous solution of Dendrimer (1 mM) containing 0.15 M N-(3-dimethylaminopropyl)-N'-ethyl carbodiimidehydrochloride (EDC) and 0.03 M N-hydroxy sulfosuccinimide (S-NHS) was prepared and left aside for 1 hr. The activated solution of Dendrimer was drop casted on PMA/AT/G/GCE and left for 1 hr., followed by washing with double distilled water to obtain the DEN-PMA/AT/G/GCE. Further, Ab-CRP was covalently immobilized on the DEN-PMA/AT/G/GCE electrode by drop casting 10  $\mu\text{L}$  of 100  $\mu\text{g mL}^{-1}$  Ab-CRP on the electrode surface, for an overnight period at 4 °C, followed by washing with PBS and drying with  $\text{N}_2$  gas flow to obtain a bioelectrode. The bioelectrode was then incubated in 0.1% bovine serum albumin (BSA) to block the nonspecific binding sites on the DEN as well as on the AT/G surface, followed by washing in PBS and dried under  $\text{N}_2$  gas flow and stored at 4°C.

## **2.9 CRP**

C-reactive protein (CRP) is an acute phase pentameric plasma protein synthesized by liver [22], consisting of five identical homologous subunits which are non-covalently associated in a cyclic form and it is widely accepted as a biomarker of cardiovascular disease and inflammation [23-25]. This acute phase protein is normally present as a constituent of plasma; levels in plasma are less than 2  $\text{mg L}^{-1}$  for healthy individuals, but increase up to many folds during acute myocardial infarction (AMI). Thus reliable and early quantification of CRP concentrations is greatly appreciated for accurate implementation of therapeutic interventions before and after AMI occurrence for monitoring the status of AMI patients. The American Heart Association and the United States Centre for Disease Control have suggested three different levels of CRP concentrations for the evaluation of cardiovascular disease risk [26-27]: CRP concentration less than 1 $\text{mg L}^{-1}$  represents a low risk state; concentration between 1 and 3  $\text{mg L}^{-1}$  is considered as an average risk state and any concentration above 3  $\text{mg L}^{-1}$  represents a high risk state. Currently, a number of CRP testing methods are available in clinical laboratories, such as nephelometric[28], turbidimetric [29], and the enzyme-linked immunosorbent assay (ELISA) kits[30]. However, these methods are not appropriate for the clinical practice as they are time-consuming, cost-ineffective, and prone to false negatives [31].CRP quantification methods based on surface plasmon resonance (SPR) [32], microfluidics [33], and electrochemistry [34], have been developed during the past few years. Among these, electrochemical assay offers the advantage of

low cost and high sensitivity [35-37]. Recently, a number of CRP assays by electrochemical impedance spectroscopy (EIS) have been reported [38-39].

## 2.10 Instrumentation

In recent years, electrochemistry has acquired increasing importance in new applications, to name just some of them biosensors, fuel cells and solar cells. The instrument potentiostat / galvanostat 302 M Autolab represents the state of the most comprehensive and advanced electrochemical instrumentation and can be used for virtually all electrochemical applications.

In fact, one of the most important features of this tool electrochemical Autolab is modularity. The basic instrument is a potentiostat / galvanostat, then with all the basic electrochemical techniques such as, cyclic voltammetry, differential pulse voltammetry, square wave voltammetry, coulometry, chronoamperometry, etc. The instrument can be further adapted to your needs by adding one or more of the modules available in a manner to increase the possibilities for application in various fields. The base module 302N is implemented with a module FRA 32M for electrochemical impedance measurements that allow electrochemically characterize the materials in a more general manner possible, as for example to assess the changes of surface or to study interactions with biological molecules and reactions and kinetics electron-transfer and not only, as is well known, in studies of corrosion.



**Figure 15: Photograph of autolab instrument model no. PGSTST302N**

The other module that implements and completes the system is a module EQCM. Using this module EQCM, one determines the ratio between the mass change of the surface of the electrode during an electrochemical reaction and the total charge involved. This technique is very useful in the study not only of redox reactions or reactions of electroplating, but also to assess both the operation of sensors and biosensors, that the variations introduced on the electrode surface during operation of the sensor, but also to follow changes in the biological material used in the case of a biosensor.

**CHAPTER-3**  
**RESULT AND DISCUSSION**



### **3.1 Electrochemical Characterization of the Bioelectrode**

CV is an efficient and versatile technique which allows probing the features of a modified electrode surface. The alteration in peak current and the separation of peak potentials in CVs at various stages of surface modification are theoretically linked to electron transfer rate constant. To explore the electrochemical behavior of the GCE and probe-modified GCE, CV was performed in a PBS solution (pH 7.4; 0.1 M KCl) containing a mixture of 2 mM  $K_3[Fe(CN)_6]$  and 2 mM  $K_4[Fe(CN)_6]$  as a redox probe at a scan rate of  $50 \text{ mVs}^{-1}$ . The bare GCE shows a quasi-reversible CV with a peak-to-peak separation between the oxidation and reduction potentials ( $\Delta V_p$ ) of 76 mV. The electrochemical behavior of CVD grown graphene-modified GCE exhibited an irreversible CV of an almost flat nature. This is attributed to the pristine crystalline nature of the graphene attached on GCE causing sluggish electron transfer at the electrode surface. The electrochemical behavior of the graphene is strongly dependent on the presence of defects on its surface microstructure. To enhance the electrocatalytic activity and to make the electrode surface permeable to redox probe, we treat graphene to create edge plane defects. This effect of treatment of graphene on its electrochemical behavior is well evident from CV. A quasi-reversible CV with a peak-to-peak separation between the oxidation and reduction potentials of 61 mV with significantly enhanced peak currents was observed for AT/G/GCE with respect to bare GCE and G/GCE due to an enhanced heterogeneous electron transfer at the edge planes. The anodization of graphene on GCE produces oxygenated groups on its surface which contributed to an increased capacitive charging current. This anodization has created strain on the  $sp^2$ -bonded lattice because of transition to  $sp^3$  bonding with oxygen species that has resulted in the formation of edge plane defects. Contrary to this result, a decrease in the peak current and increase in the peak-to-peak redox potential were obtained for the PMA/AT/G/GCE. This may be attributed to the repulsive interaction between the lone pair of nitrogen of primary amino group of PMA and the negatively charged  $[Fe(CN)_6]^{3-/4-}$  redox probe. The CV redox peak current further decreased with the attachment of Dendrimer nanoparticles on the PMA/AG/GCE because of the repulsive interaction of  $COO^-$  groups of Dendrimer with the anionic probe at the electrode solution interface.[40]

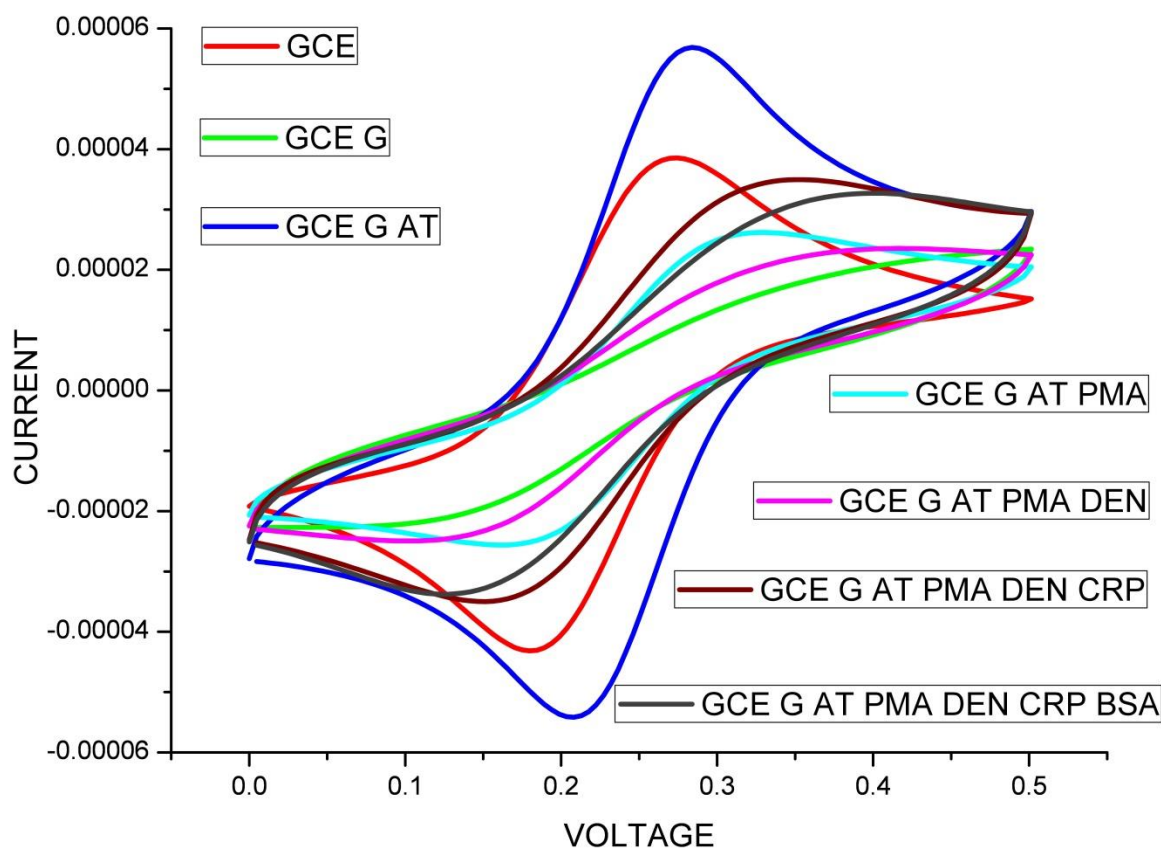


**Figure 16: Cyclic voltammetry of the matrix**

### **3.2 EIS of the matrix Ab-CRP/DEN-PMA/ AT/G/GCE**

The cyclic voltammetry results were further authenticated by EIS measurements which were used to investigate changes on the electron transfer process at electrode solution interface through the immunosensor fabrication. Electrochemical impedance spectroscopy was employed to characterize the fabrication of the immunosensor by studying the interface properties of the modified electrode. The typical impedance spectrum is represented as Nyquist plot, and it includes a semicircle part at higher frequencies corresponding to electron transfer limited process and a linear part at lower frequencies corresponding to diffusion-limited process. The diameter of the semicircle in the Nyquist plot is equal to the electron transfer resistance which reflects the electron transfer kinetics of the redox probe at the electrode surface.

The EIS experimental data obtained during the stepwise fabrication of the bioelectrode were fitted to Randle's equivalent circuit, and the corresponding values of the EIS parameters are given in Table 1 and Table 2. CPE is used in place of pure capacitor ( $C_{dl}$ ) to account for the effect of the roughness of electrode surface and represented by

$$CPE = Y_0^{-1}(j\omega)^{-n}$$

where  $j$  is the imaginary number,  $Y_0$  is the admittance of an ideal capacitor,  $\omega$  is the angular frequency, and  $n$  explains the extent of deviation of the semicircle from its ideal form and is attributed to the heterogeneity of the electrode surface. CPE greatly depends on the insulating features at the electrode–solution interface, on the surface area of the electrode, and on the thickness of the separation layer. CPE can represent capacitance ( $C=Y_0$ ) for  $n=1$ , a resistance ( $R=1 / Y_0$ ) for  $n=0$ , an inductance ( $L=1 / Y_0$ ) for  $n=-1$ , and a Warburg impedance for  $n=1 / 2$ . In our case, the value of  $n$  for distinctly modified electrodes is less than 1, suggesting the pseudo-capacitive behavior of the electrode. A negligible change in the value of solution resistance was observed by modifications on the electrode surface so it has been ignored. The impedance spectrum corresponding to the stepwise modification processes is shown in Fig.16. It was observed that the EIS of the bare GCE displayed an electron transfer resistance of  $15.51 \Omega\text{cm}^2$ . The electrode after modification with graphene showed electron transfer resistance of  $274.41 \Omega\text{cm}^2$ , indicating the successful attachment of pristine graphene on GCE blocking the redox electron transfer at the electrode surface. The EIS showed a very small  $R_{et}$  of  $8.65 \Omega\text{cm}^2$  with almost a straight line at low frequencies after anodization of the graphene, suggesting that the electrode reaction was only controlled by diffusion-limited process. This corresponds to an enhanced heterogeneous electron transfer rate constant, which may be resulted due to the edge plane defects at the anodized graphene surface. After the deposition of PMA on AT/G/ GCE, the  $R_{et}$  increased to  $126.07 \Omega\text{cm}^2$  due to a repulsive interaction between the primary amine and anionic redox probe at the electrode–solution interface. A further increase in  $R_{et}$  value to  $218.33 \Omega\text{cm}^2$  was obtained after the dendrimer functionalization of the PMA/AT/G/GCE due to the repulsion between the negatively charged carboxyl moiety and the redox probe. There is decrease in  $R_{et}$  values i.e  $84.77 \Omega\text{cm}^2$  was observed after the modification of the DEN-PMA/ AT/G/GCE with Ab-CRP i.e Ab-CRP/DEN-PMA/ AT/G/GCE and then further increase in  $R_{et}$  values i.e  $131.6 \Omega\text{cm}^2$  due to passivation with a blocking reagent BSA.

**Table 1** EIS characteristics parameter at various stages of surface modification of the electrode of GCE

Type of Electrodes	$\Delta E_p$ (mV)	$R_{ct}$ ( $\Omega\text{cm}^2$ )	CPE		$k^0(10^{-4})$ ( $\text{m s}^{-1}$ )	$Z_w (10^{-5})$ ( $\Omega\text{cm}^2$ )	$\chi^2$ ( $\times 10^{-2}$ )
			$Y_0$ ( $\mu\text{Fcm}^{-2}$ )	$n$			
Bare GCE	76	15.51					
G/GCE	-	274.41	0.10	.70	0.98	3.50	0.52
AT/G/GCE	61	8.659	3.01	.76	31.2	5.00	3.94
PMA/AT/G/GCE	156	126.07	2.03	.84	2.14	4.30	4.42
DEN/PMA/AG /GCE	326	218.33	2.11	.86	1.24	4.55	4.68
CRP/DEN/PMA/AG/G CE	208	84.77	2.03	.83	3.19	4.38	0.16
BSA/CRP/DENPMA/ AG/GCE	289	131.6	1.94	.84	2.05	4.48	0.14

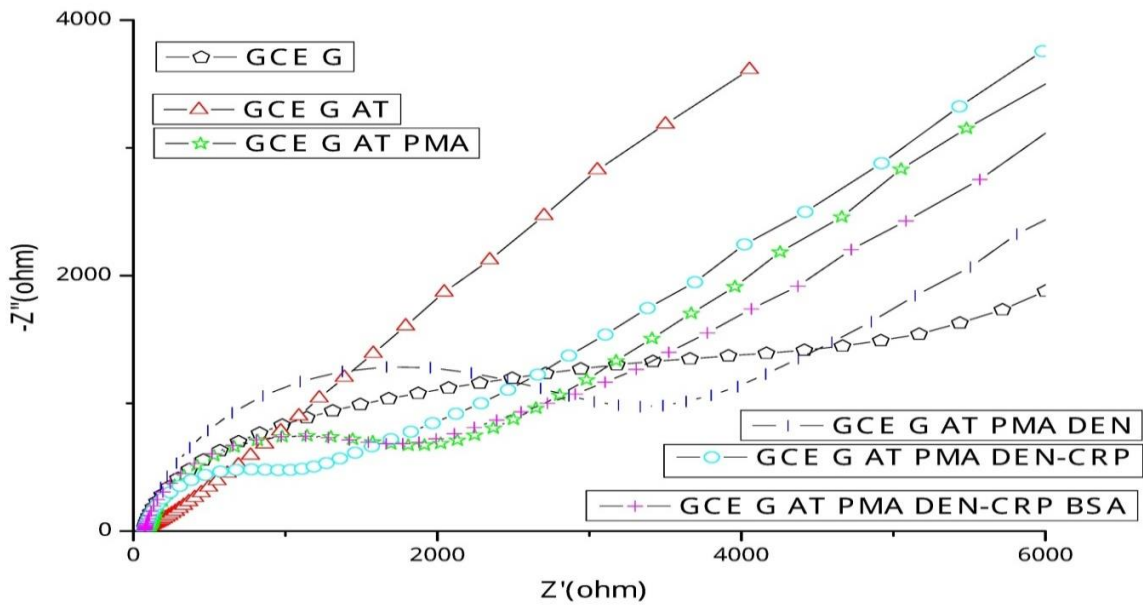


**Figure 17: Nyquist Plot of the matrix of electrode GCE**

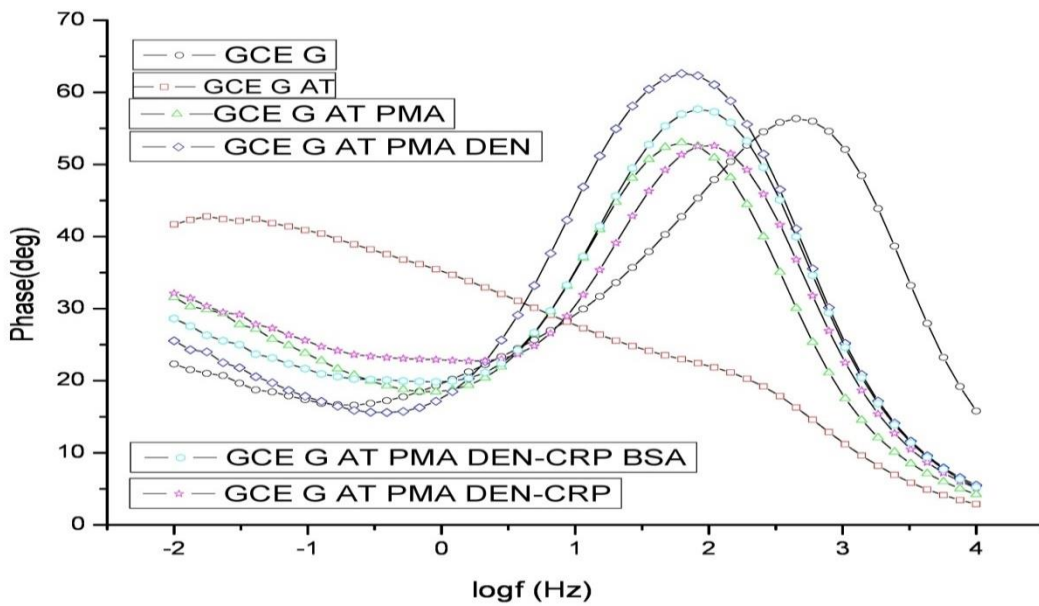


**Figure 18: Bode Plot (Phase analysis) of the matrix of electrode GCE**

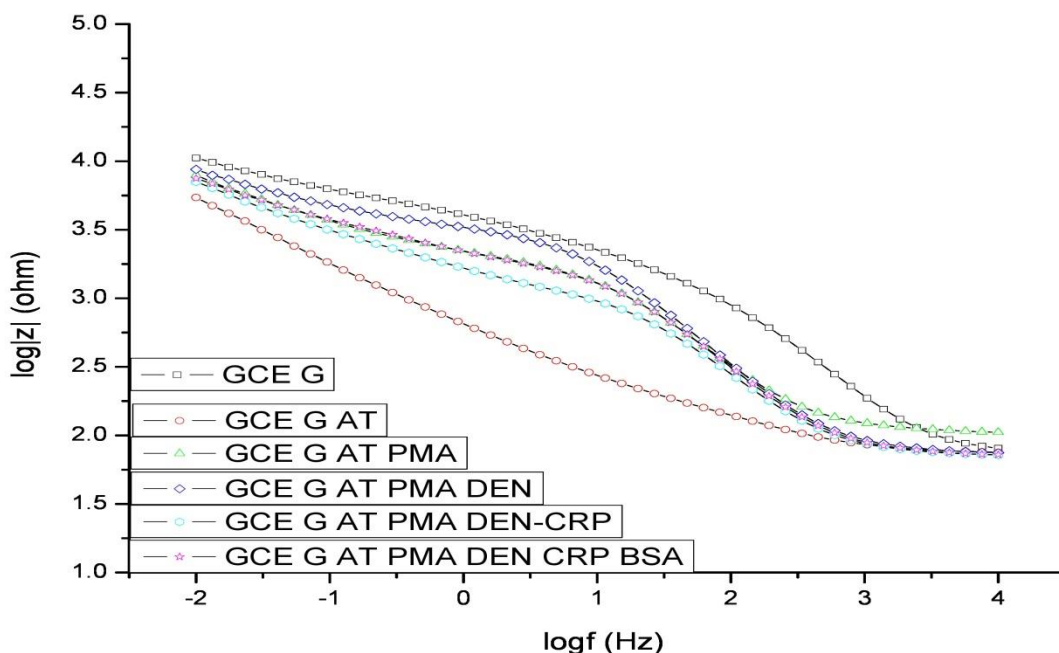


**Figure 19: Bode Plot (impedance analysis) of the matrix of electrode GCE**

### **3.3 Electrochemical Impedance Response to Ag-CRP**

Compared to other electrochemical techniques, impedance measurement offers the advantage that the impedance is measured under stationary potential conditions, as opposed to the wide potential window used in CVs. After the successful preparation of the Ab-CRP(BSA)-DEN-PMA/AT/G/GCE bioelectrode, it was applied as an EIS immunosensor for the detection of protein antigen, Ag-CRP. EIS measurements were carried out after dispensing 10  $\mu$ L sample solution of the different concentration of target Ag-CRP on the bioelectrode surface for 10 minutes, followed by washing with PBS and drying under  $N_2$  flow at room temperature. The changes in the impedance measurements on the bioelectrode were recorded with different concentration of Ag-CRP with respect to the control sample containing no antigen. Figure shows the Nyquist plot of impedance spectra of immunosensor for different concentration of Ag-CRP.

It was found that the amplitude of semicircle in the Nyquist plots gradually increased with the increasing concentration of the dispersed Ag-CRP, indicating an increasing antibody-antigen complex formation, resulting in a large electron transfer resistance at the electrode surface. The immunoreaction was further investigated by using frequency ( $f$ ) dependent Bode impedance and phase ( $\varphi$ ) curves in order to appreciate the various constituent phases of the system. The Bode plot can be divided into four different frequency domains indicative of different kinetics dominant in those regions. Observation of no significant changes in the impedance in the frequency region  $> 1$  KHz is indicative of purely resistive behavior of the bioelectrode, while the pseudocapacitive behavior is dominant in the region between 100 Hz to 1000 Hz. The region from 10 Hz to 0.1 Hz corresponds to  $R_{et}$  and below 0.1 Hz the process is mainly diffusion controlled in nature. Since, major changes were observed in  $R_{et}$  amongst the various circuit elements, it was taken as suitable sensing element for monitoring the immunoreaction towards the target Ag-CRP.

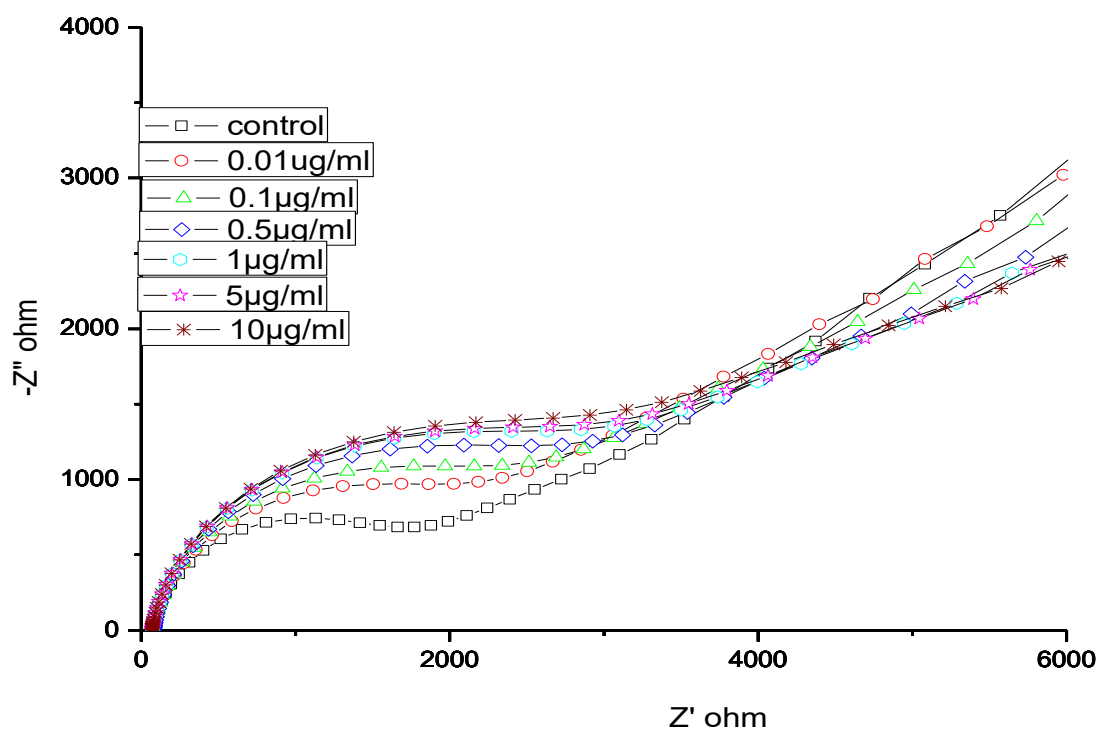


**Figure 20: Nyquist Plot response to Ag-CRP at different concentration of electrode GCE**

**Table 2** EIS characteristics parameters of the bioelectrode on immunoreaction with different concentration of target Ag-CRP GCE

Immunoreaction with [Ag-CRP]	$R_{et}$ ( $\Omega \text{ cm}^2$ )	CPE		$W_R$ ( $\Omega \text{ cm}^2$ )	$\chi^2$ ( $10^{-4}$ )	$K^o$ ( $10^{-4}$ ) ( $\text{m s}^{-1}$ )
		$Y_0$ ( $\mu\text{F cm}^{-2}$ )	$n$			
Control	131.6	1.94	.840	2.05	4.48	0.14
0.01 $\mu\text{g mL}^{-1}$	156.45	4.1	.857	4.28	9.26	1.73
0.10 $\mu\text{g mL}^{-1}$	175.91	4.0	.854	4.28	9.16	1.54
0.50 $\mu\text{g mL}^{-1}$	200.06	3.9	.850	4.24	9.32	1.35
1.00 $\mu\text{g mL}^{-1}$	216.37	3.8	.849	4.17	11.5	1.25
5.00 $\mu\text{g mL}^{-1}$	220.85	3.7	.846	4.09	13.1	1.22
10.0 $\mu\text{g mL}^{-1}$	229.60	3.6	.842	4.01	15.0	1.18

$\Delta E_p$  = redox potential;  $R_{et}$  = charge transfer resistance; CPE = constant phase element;  $k^o$  = apparent rate constant;  $Z_w$  = Warburg impedance



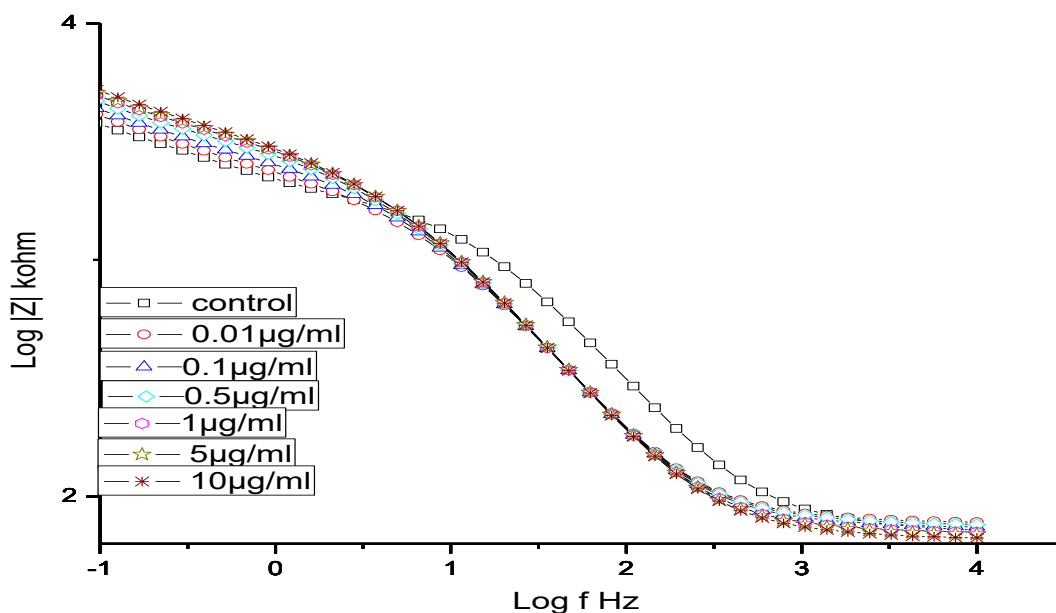


**Figure 21: Bode Plot (impedance analysis) response to Ag-CRP at different concentration of electrode GCE**

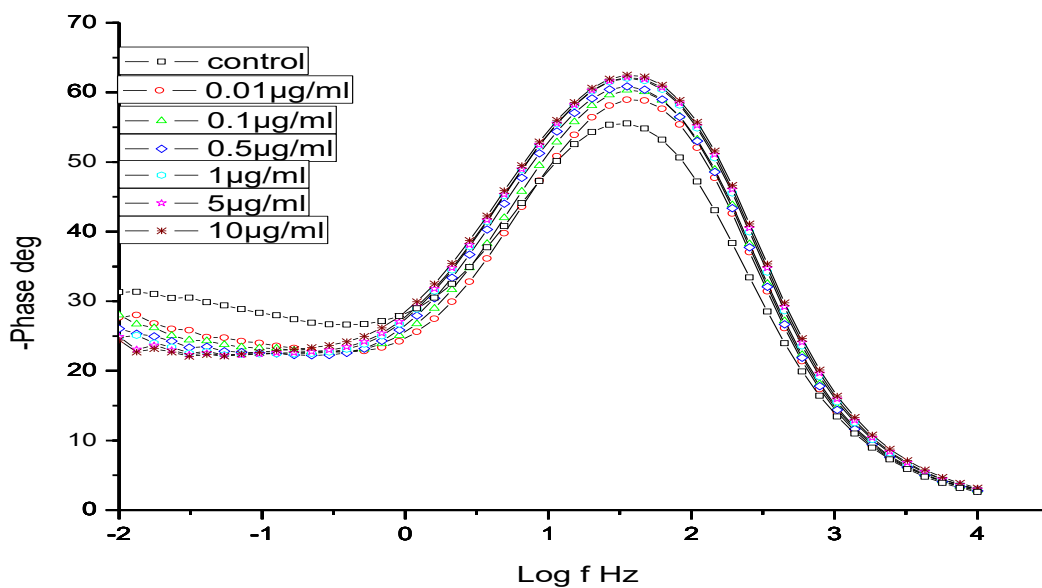


**Figure 22: Bode Plot (Phase analysis) response to Ag-CRP at different concentration of electrode GCE'**

**CHAPTER-4**  
**CONCLUSION**

## Conclusion

A simple electrochemical impedimetric immunosensor based on CVD grown graphene-DEN for the ultrasensitive detection of C-reactive protein (Ag-CRP) has been reported. The Dendrimer were covalently immobilized over anodized graphene using PMA leading to a highly uniform distribution of Dendrimer. The dendrimer provided an efficient covalent bonding of protein antibody, Ab-CRP, with high loading and good probe orientation. The immunosensor was characterized by CV and EIS. The immunosensor exhibited a linear impedimetric response to Ag-CRP in the range of  $0.01 \mu\text{g mL}^{-1}$  to  $10 \mu\text{g mL}^{-1}$  in human serum with a sensitivity of  $21.2 \Omega \text{ cm}^2$  per decade, with acceptable reproducibility and specificity for Ag-CRP.

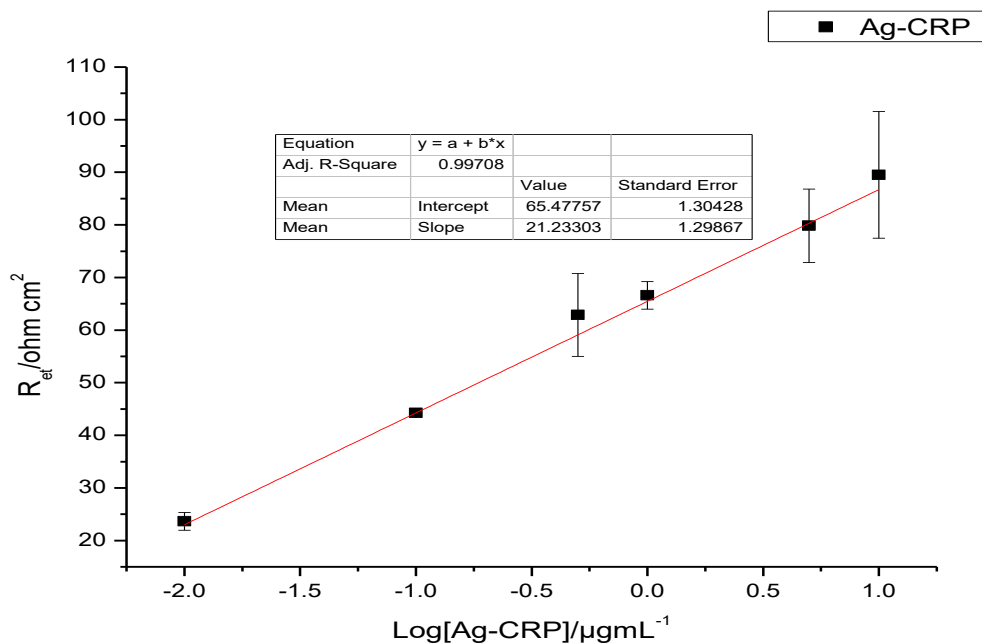


**Figure 23: Concentration-dependent Calibration curve for Ab-CRP (BSA)-DEN-PMA/AT/G/GCE**

## REFERENCES

---

- [1] U. YOGESWARAN AND S.-M. CHEN, "A REVIEW ON THE ELECTROCHEMICAL SENSORS AND BIOSENSORS COMPOSED OF NANOWIRES AS SENSING MATERIAL," SENSORS, VOL. 8, NO. 1, PP. 290–313, JAN. 2008.
- [2] T. AHUJA, I. MIR, D. KUMAR, AND RAJESH, "BIOMOLECULAR IMMOBILIZATION ON CONDUCTING POLYMERS FOR BIOSENSING APPLICATIONS," BIOMATERIALS, VOL. 28, NO. 5, PP. 791–805, FEB. 2007.
- [3] M. FERRARI, R. BASHIR, AND S. WERELEY, EDS., "BIOMEMS AND BIOMEDICAL NANOTECHNOLOGY," 2006.
- [4] J.P. ALARIE AND T.VO-DINH. POLYCYC. AROMAT. COMPD., 8:45, 1996.
- [5] S.L.R. BARKER, R. KOPELMAN, T.E. MEYER, AND M.A. CUSANOVICH. ANAL. CHEM., 70:971, 1998.
- [6] B.M. CULLUM, G.D. GRIFFIN, AND T. VO-DINH. ANAL. BIOCHEM., 1999.
- [7] D. DIAMOND. (ED.). CHEMICAL AND BIOLOGICAL SENSORS. WILEY, NEW YORK, 1998.
- [8] N. ISOLA, D.L. STOKES, AND T. VO-DINH. ANAL. CHEM., 70:1352, 1998.
- [9] T. VO-DINH, N. ISOLA, J.P. ALARIE, D. LANDIS, G.D. GRIFFIN, AND S. ALLISON. INSTRUM. SCI. TECHNOL., 26:503, 1998.
- [10] T. VO-DINH, K. HOUCK, AND D.L. STOKES. ANAL. CHEM., 33:3379, 1994.
- [11] T. VO-DINH, B.M. CULLUM, J.P. ALARIE, AND G.D. GRIFFIN. J. NANOPART. RES., (IN PRESS).
- [12] T. VO-DINH, G.D. GRIFFIN, AND K.R. AMBROSE. APPL. SPECTROSC., 40:696, 1986.
- [13] T. VO-DINH, B.G. TROMBERG, G.D. GRIFFIN, K.R. AMBROSE, M.J. SEPANIAC, AND E.M. GARDENHIRE. SUPPL.SPECTROSC., 41:735, 1987.
- [14] BRAGUGLIA CM. BIOSENSORS: AN OUTLINE OF GENERAL PRINCIPLES AND APPLICATION. CHEMICAL AND BIOCHEMICAL ENGINEERING QUARTERLY. 1998;12(4):183-90.
- [15] C. GALAN-VIDAL, J. MUNOZ, C. DOMINGUEZ, AND S. ALEGRET. SENSOR. ACTUAT. B-CHEM., 53:257, 1998.
- [16] J.G. HACIA, S.A.WOSKI, J. FIDANZA, K. EDGEMON, G. MCGALL, S.P.A. FODOR, AND F.S. COLLINS. NUCLEIC ACIDS RES., 26:4975, 1998.

- [17] F. TOBALINA, F. PARIENTE, L. HERNANDEZ, H.D. ABRUNA, AND E. LORENZO. ANAL. CHIM. ACTA, 395:17, 1999
- [18] M. MINUNNI, M. MASCINI, R.M. CARTER, M.B. JACOBS, G.J. LUBRANO, AND G.C. GUILBAULT. ANAL. CHIM. ACTA,325:169, 1996.
- [19] T. THUNDAT, P.I. ODEN, AND R.J. WARMACK. MICROSCALE THERMOPHYS. ENG., 1:185, 1997.
- [20] B. D. MALHOTRA, R. SINGHAL, A. CHAUBEY, S. K. SHARMA, AND A. KUMAR, "RECENT TRENDS IN BIOSENSORS," CURRENT APPLIED PHYSICS, VOL. 5, NO. 2, PP. 92–97, FEB. 2005.
- [21] DIAMOND, D. (ED.), PRINCIPLES OF CHEMICAL AND BIOLOGICAL SENSORS, WILEY, NEW YORK
- [22] PEPYS, M. B. & HIRSCHFIELD, G. M. (2003). JOURNAL OF CLINICAL INVESTIGATION, 111, 1805.
- [23] MAY A, WANG TJ, EXPERT REVIEW OF MOLECULAR DIAGNOSTICS 7: 793-804 (2007).
- [24] MILLER VM, REDFIELD MM, McCONNELL JP, CURRENT VASCULAR PHARMACOLOGY 5: 15-25 (2007).
- [25] MYGIND ND, HARUTYUNYAN MJ, MATHIASSEN AB, RIPA AB, THUNE RS, GOTZE JJ, JOHANSEN JP, KASTRUP JS, GRP J, C.T INFLAMMATION RESEARCH 60: 281-287 (2011).
- [26] KUSHNER I, SEHGAL AR, ARCHIVES OF INTERNAL MEDICINE 162: 867-869 (2002).
- [27] BENZAQUEN LR, YU H, RIFAI N, CRITICAL REVIEWS IN CLINICAL LABORATORY SCIENCES 39: 459-497 (2002).
- [28] ROBERTS WL, SEDRICK R, MOULTON L, SPENCER A, RIFAI N, CLINICAL CHEMISTRY 46: 461-468 (2000).
- [29] ROBERTS WL, MOULTON L, LAW TC, FARROW G, COOPER-ANDERSON M, SAVORY J, RIFAI N, CLINICAL CHEMISTRY 47: 418-425 (2001).
- [30] MACY EM, HAYES TE, TRACY RP, CLINICAL CHEMISTRY 43: 52-58 (1997).
- [31] PEARSON TA, MENSAH GA, HONG YL, SMITH SC, CIRCULATION 110: 543-544 (2004).
- [32] HU WP, HSU HY, CHIOU A, TSENS KY, LIN HI, CHANG GL, CHEN SJ, BIOSENS. BIOELECTRON. 21: 1631–1637 (2006).
- [33] LEE WB, CHEN YH, LIN HI, SHIESH SC, LEE GB, SENSORS AND ACTUATORS B: CHEMICAL 157: 710–721 (2011).

- [34] BUCH M, RISHPON J, ELECTROANALYSIS 20: 2592–2594 (2008).
- [35] PEI, R. J., CHENG, Z. L., WANG, E. K. & YANG, X. R. (2001). BIOSENSORS AND BIOELECTRONICS, 16, 355.
- [36] KATZ, E. & WILLNER, I. (2003). ELECTROANALYSIS, 15, 913.
- [37] TANG, D., YUAN, R., CHAI, Y., DAI, J., ZHONG, X. & LIU, Y. (2004). BIOELECTROCHEMISTRY, 65, 15.
- [38] RAJESH, SHARMA V, TANWAR VK, BIRADAR AM, SENSOR LETT. 8: 362-369 (2010).
- [39] GUPTA RK, PERIYAKARUPPAN A, MEYYAPPAN M, KOEHNE JE, BIOSENS. BIOELECTRON. 59: 112-119 (2014).
- [40] SINGAL, SHOBHITA AND BIRADAR, A.M. AND MULCHANDANI, ASHOK AND RAJESH (2014) ULTRASENSITIVE ELECTROCHEMICAL IMMUNOSENSOR BASED ON PT NANOPARTICLE-GRAPHENE COMPOSITE. APPLIED BIOCHEMISTRY AND BIOTECHNOLOGY, 174 (3). 971-983 . ISSN 0273-2289